

Selective activation of prodrugs in breast cancer using metabolic glycoengineering and the tetrazine ligation bioorthogonal reaction

Article

Published Version

Creative Commons: Attribution 4.0 (CC-BY)

Open Access

Mitry, M. M.A., Dallas, M. L. ORCID: https://orcid.org/0000-0002-5190-0522, Boateng, S. Y., Greco, F. and Osborn, H. M. I. ORCID: https://orcid.org/0000-0002-0683-0457 (2024) Selective activation of prodrugs in breast cancer using metabolic glycoengineering and the tetrazine ligation bioorthogonal reaction. Bioorganic Chemistry, 147. 107304. ISSN 1090-2120 doi: 10.1016/j.bioorg.2024.107304 Available at https://centaur.reading.ac.uk/115843/

It is advisable to refer to the publisher's version if you intend to cite from the work. See Guidance on citing.

To link to this article DOI: http://dx.doi.org/10.1016/j.bioorg.2024.107304

Publisher: Elsevier

All outputs in CentAUR are protected by Intellectual Property Rights law, including copyright law. Copyright and IPR is retained by the creators or other copyright holders. Terms and conditions for use of this material are defined in



the End User Agreement.

www.reading.ac.uk/centaur

CentAUR

Central Archive at the University of Reading Reading's research outputs online

ELSEVIER

Contents lists available at ScienceDirect

Bioorganic Chemistry

journal homepage: www.elsevier.com/locate/bioorg





Selective activation of prodrugs in breast cancer using metabolic glycoengineering and the tetrazine ligation bioorthogonal reaction

Madonna M.A. Mitry ^{a,b}, Mark L. Dallas ^a, Samuel Y. Boateng ^c, Francesca Greco ^{a,*}, Helen M. I. Osborn ^{a,*}

- ^a Reading School of Pharmacy, University of Reading, Whiteknights, Reading RG6 6AD. UK
- ^b Dept. of Pharmaceutical Chemistry, Faculty of Pharmacy, Ain Shams University, Cairo 11566, Egypt
- ^c School of Biological Sciences, University of Reading, Whiteknights, Reading RG6 6UB, UK

ARTICLE INFO

Keywords: Bioorthogonal chemistry Tetrazine ligation Breast cancer Metabolic glycoengineering Prodrug activation

ABSTRACT

Increasing the selectivity of chemotherapies by converting them into prodrugs that can be activated at the tumour site decreases their side effects and allows discrimination between cancerous and non-cancerous cells. Herein, the use of metabolic glycoengineering (MGE) to selectively label MCF-7 breast cancer cells with tetrazine (Tz) activators for subsequent activation of prodrugs containing the trans-cyclooctene (TCO) moiety by a bioorthogonal reaction is demonstrated. Three novel Tz-modified monosaccharides, Ac₄ManNTz 7, Ac₄GalNTz 8, and Ac₄SiaTz 16, were used for expression of the Tz activator within sialic-acid rich breast cancer cells' surface glycans through MGE. Tz expression on breast cancer cells (MCF-7) was evaluated versus the non-cancerous L929 fibroblasts showing a concentration-dependant effect and excellent selectivity with ≥35-fold Tz expression on the MCF-7 cells versus the non-cancerous L929 fibroblasts. Next, a novel TCO-N-mustard prodrug and a TCOdoxorubicin prodrug were analyzed in vitro on the Tz-bioengineered cells to probe our hypothesis that these could be activated via a bioorthogonal reaction. Selective prodrug activation and restoration of cytotoxicity were demonstrated for the MCF-7 breast cancer cells versus the non-cancerous L929 cells. Restoration of the parent drug's cytotoxicity was shown to be dependent on the level of Tz expression where the Ac₄ManNTz 7 and Ac₄GalNTz 8 derivatives (20 μM) lead to the highest Tz expression and full restoration of the parent drug's cytotoxicity. This work suggests the feasibility of combining MGE and tetrazine ligation for selective prodrug activation in breast cancer.

1. Introduction

Chemotherapy is an integral part of cancer treatment, however serious side effects are often evident due to the inability of the cytotoxic components to discriminate between normal and cancer cells [1–3]. Modification of non-specific cytotoxic chemotherapies into less potent prodrugs, that are specifically activated at the required tumour site, is a valuable and widely reported approach within targeted medicinal chemistry approaches for cancer [4–6]. However, the most commonly applied prodrug strategies rely on enzymatic activation by local or tumour-upregulated enzymes and hence their clinical impact can be compromised by non-specific activation at non-tumour sites (i.e. off-site activation) or heterogeneity in the expression level of the targeted tumour-specific enzyme [7,8]. An alternative approach has seen the use

of bioorthogonal reactions [9] for prodrug activation due to their biocompatibility, versatility, high selectivity, and click-and-release mechanisms [10–12]. A range of bioorthogonal reactions have been used in prodrug activation including the 1,3-dipolar cycloadition of an azide and a strained*trans* cyclooctenol [13], Pd-mediated bond cleavage [14], Staudinger ligation reaction [15] and the Inverse Electron Demand Diels-Alder (IEDDA) reactions [10]. However, to allow selective activation of the prodrug at the required site of action, targeting approaches must be used to deliver the bioorthogonal activators to the required location, for example using active targeting, passive targeting, or metabolic glycoengineering (MGE) whereby chemically-modified monosaccharides are used to intercept cell surface glycans' natural biosynthesis pathway to allow expression of these unnatural chemical moieties on cells' surfaces within glycoproteins [16].

E-mail addresses: m.m.adeebmitry@pgr.reading.ac.uk (M.M.A. Mitry), m.dallas@reading.ac.uk (M.L. Dallas), s.boateng@reading.ac.uk (S.Y. Boateng), f.greco@reading.ac.uk (F. Greco), h.m.i.osborn@reading.ac.uk (H.M.I. Osborn).

^{*} Corresponding authors.

MGE is an appealing strategy in cancer targeting because it relies on a differential glycosylation state between cancerous and non-cancerous cells due to the altered expression levels of glycosyltransferases and glycosidases including the upregulation of a glycosyltransferase called sialyl transferase [17]. Sialyl transferase is an enzyme that adds sialic acid residues to crown the terminal oligosaccharide chains in cell membrane glycoproteins and glycolipids. Its upregulation leads to a hypersialylation condition in tumour cells in which some glycans known as Tumour-Associated Carbohydrate Antigens (TACAs) are overexpressed [18,19]. N-Acetylneuraminic acid (Sialic acid) is the main component of these TACAs, especially polysialic acid (PSA) that is overexpressed in breast cancer [20]. Mannosamine, galactosamine, and sialic acid derivatives have been previously reported to intercept PSA biosynthesis in breast cancer cells hence engineering chemical reporters on their cell surfaces [21,22].

For our prodrug activation strategy, we selected a subclass of the IEDDA bioorthogonal reactions, specifically the tetrazine ligation. This is a click-to-release reaction that involves a reaction between a dienophile (trans-cyclooctene (TCO)) and a diene (1,2,4,5-tetrazine (Tz)) to give fused dihydropyridazines that undergo isomerization and release the drug payload attached to the allyl position of the TCO under fast kinetics [23]. Cancer chemotherapies such as doxorubicin and monomethyl auristatin E (MMAE) have been converted to TCO-prodrugs for subsequent activation by various Tz activators [24-26]. However, active targeting using antibody-conjugated TCO-prodrugs and passive targeting using polymers and nanoparticles have most frequently been reported for selective targeting of the TCO and Tz components for selective activation of TCO-prodrugs [24,25]. MGE has received very little attention for the delivery of the Tz components for selective activation of TCO-prodrugs at tumours, despite its proven value for delivery of activators for complementary prodrug strategies, such as reported by our group for selective prodrug activation in breast cancer using the Staudinger ligation reaction [22]. MGE presents potential advantages over other cancer-targeting strategies including active targeting. For example, as it does not rely on the natural expression of endogenous protein receptors, it addresses limitations that arise from the heterogeneous expression of tumour biomarkers. Moreover, as the strategy exploits the biosynthesis of natural glycans, it can lead to high expression levels of the moiety required for activation of the prodrug, leading to a more efficient prodrug activation approach. When compared with antibody approaches for delivering the bioorthogonal moieties, MGE is also likely to afford preferential toxicity profiles with lower immunogenicity risks. Finally, chemical modification of the monosaccharides to incorporate the bioorthogonal components is more facile compared with modification of the antibodies, where their binding affinities can be significantly altered following chemical modification [27–29].

Herein, we disclose our results concerning MGE and the tetrazine ligation bioorthogonal reaction, for selective prodrug activation in human breast cancer cells. To the best of our knowledge, only one study has very recently reported the use of MGE for Tz expression on cancer cells' surfaces for imaging and therapy applications [30]. We further extend and optimize the approach by probing the selectivity of the approach using a series of novel Tz-modified monosaccharides for MGE and subsequently determine the Tz expression level on breast cancer cells versus non-cancerous fibroblast cells. We also consider the use of lower concentrations of the Tz-modified monosaccharides than previously reported. Finally, we challenge our hypothesis using an additional chemotherapeutic prodrug (i.e. TCO-N-mustard) to that reported previously (i.e. TCO-doxorubicin), to comprehensively validate the approach for potential application against breast cancer. The overall two-step selective prodrug activation strategy using a combined bioorthogonal chemistry/MGE approach is summarised in Fig. 1.

First, for the activator part of the approach (Fig. 1), the design, synthesis, and characterization of novel Tz-modified monosaccharide derivatives that are hypothesized to allow the Tz activator expression within tumour cell surface glycans through MGE are reported. Mannosamine, and to a lesser extent, galactosamine and sialic acid (Neu5Ac) derivatives are known to be used as metabolic precursors for MGE and interception of cells' surfaces glycans biosynthesis [31–33], therefore they were selected for derivatization with Tz. A 1,2,4,5-tetrazine moiety with 3-benzyl and 6-methyl substituents was chosen to derivatize the three monosaccharides as it has previously shown to be a suitable Tz molecule for a click-to-release activation of TCO-prodrugs where it shows a good balance between reactivity and stability [24,25].

With respect to the prodrug part of the approach (Fig. 1), it has been reported that the reactivity of the TCO-prodrug (with Tz activators) is

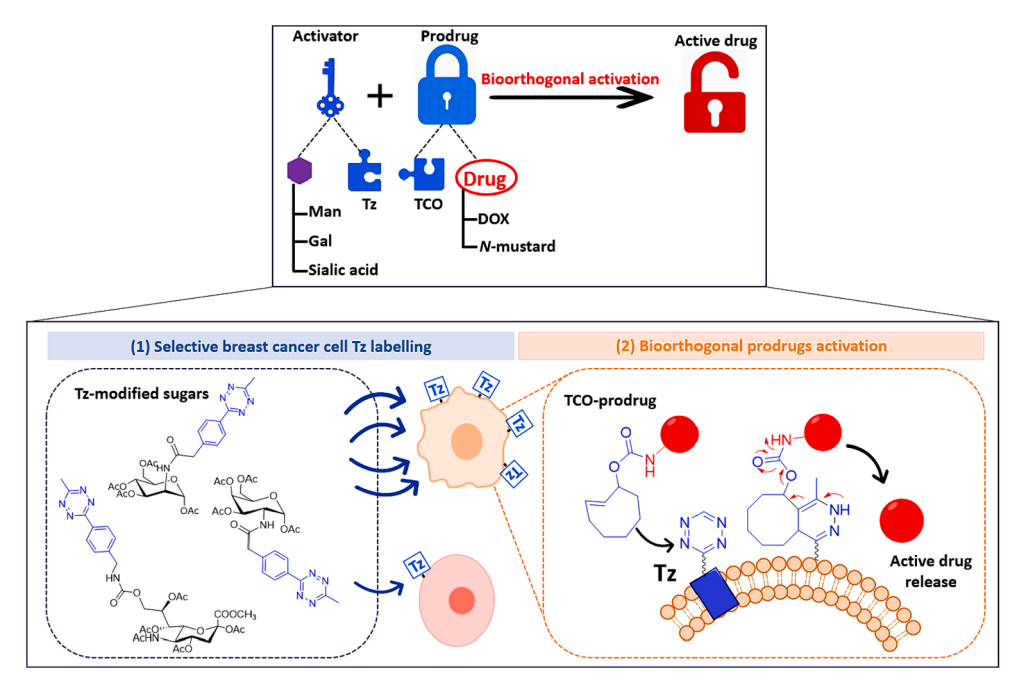


Fig. 1. Schematic illustration of targeted bioorthogonal prodrug activation strategy in breast cancer. (1) Selective labeling of MCF-7 breast cancer cells' surfaces with Tz-modified monosaccharides vs non-cancerous fibroblasts leading to Tz expression. (2) Targeted activation of TCO-prodrugs at breast cancer cells *via* Tz ligation reaction with the expressed Tz moieties.

Fig. 2. Mechanism of action of doxorubicin (a) and N-mustards (b). Functional groups essential for activity highlighted through light blue shading.

affected by the stereochemistry of the carbamate-linked prodrug. The axially positioned carbamate-linked prodrug is more reactive than the equatorially positioned carbamate-linked prodrug, and the *trans*-isomer is more reactive than the *cis*-isomer [23]. Therefore, a *trans*-cyclooctene 4-nitrophenyl carbonate starting material (axial isomer) was used herein for the synthesis of the TCO-prodrugs. Doxorubicin and *N*-mustard were selected as the cytotoxic moieties, due to their known high effectiveness

as chemotherapies for various cancer types including breast cancer [34,35]. Specific functional groups within the parent drugs that are essential for activity were masked when forming the prodrugs, in order to remove the cytotoxic activity of the parent drug until activation. The amino group within the daunosamine ring in doxorubicin is essential for DNA intercalation that prevents DNA replication (Fig. 2a) [36]. Therefore masking this amino group through a carbamate linkage to the TCO

(i) N-Hydroxy succinimide, DIC, CHCl₃, N_2 atmosphere, RT, 4 h, 70%; (ii) TEA, MeOH, sonication at 50 °C for 30 minutes then stir under N_2 atmosphere, RT, overnight, 44% and 50%; (iii) Acetic anhydride, pyridine, N_2 atmosphere, RT, overnight 67% and 74%.

moiety was hypothesized to decrease its cytotoxicity. For *N*-mustards, the availability of the lone pair on the bis(2-chloroethyl)amino group is essential for DNA binding and cross-linking of the DNA strands (Fig. 2b) [34,37]. Forming a carbamate-linked TCO moiety at the *para*-position of the phenyl ring was hypothesized to decrease the lone pair availability and thereby decrease its cytotoxicity. The synthesis and characterization of the novel TCO-*N*-mustard prodrug along with the previously reported TCO-doxorubicin prodrug [23], is therefore described.

Next, the validity of the approach is evaluated *in vitro*. Specifically, the Tz expression level within cell surface glycans in MCF-7 cells and L929 fibroblasts is evaluated by western blotting and confocal microscopy imaging, to determine the feasibility of selectively labelling the breast cancer cells with the Tz. Finally, the activation of the TCO-prodrugs *via* ligation with the Tz component is validated using MCF-7 breast cancer cells and the L929 fibroblasts that had been subjected to MGE, to further probe the selectivity of the activation. Taken together, this work contributes to the emerging area of combining MGE for Tz expression on breast cancer cells, and bioorthogonal tetrazine ligation for subsequent prodrug activation, and is the first report to demonstrate the selectivity of this targeting approach.

2. Results and discussion

2.1. Synthesis of the Tz-activators and the TCO-prodrugs

In order to test our hypothesis that MGE could be used to express the Tz activator moiety onto the cancer cells' surfaces, three Tz-modified

monosaccharides (i.e. mannosamine, galactosamine, and sialic acid) were prepared. N-Tz mannosamine derivative $Ac_4ManNTz$ 7 and N-Tz galactosamine derivative $Ac_4GalNTz$ 8 were synthesized according to Scheme 1. 9-Tz sialic acid derivative Ac_4SiaTz 16 was synthesized according to Scheme 2. The small library of the Tz-modified monosaccharides 7, 8, and 16 were purified by column chromatography and characterized using 1H and ^{13}C NMR spectroscopy, and mass spectrometry.

For the synthesis of the N-Tz mannosamine and the N-Tz galactosamine derivative, 2-(4-(6-methyl-1,2,4,5-tetrazin-3-yl)phenyl)acetic acid 1 was first converted to its N-hydroxy succinimide derivative 2 [38] to facilitate its reaction with D-mannosamine and D-galactosamine yielding the N-Tz mannosamine ManNTz 5 and N-Tz galactosamine GalNTz 6 derivatives in 44 % and 50 %, respectively. 1,3,4,6 Acetylation of mannosamine and galactosamine derivatives is reported to increase their lipophilicity and thereby their cellular uptake [39]. Therefore, acetylation of ManNTz 5 and GalNTz 6 using acetic anhydride in pyridine was carried out to yield $Ac_4ManNTz$ 7 and $Ac_4GalNTz$ 8 in 67 % and 74 %, respectively.

For the synthesis of the Tz-sialic acid derivative, a protecting group strategy was employed to mask all positions on the sialic acid except for the free hydroxyl group at position 9. This strategy starts with esterification of the carboxylic group at position 1 in the *N*-acetyl-neuraminic acid 9 to yield its methyl ester 10, followed by the protection of primary alcohol functionality at position 9 using *tert*-butyl dimethylsilylchloride (TBDMSCl) to give the 9-O-TBDMS-Neu5Ac methyl ester 11 in 59 % yield. Then acetylation was performed to yield the fully protected sialic

(i) TFA, dry MeOH, RT, overnight, 86%; (ii) TBDMSCI, dry pyridine, N₂ atmosphere, RT, overnight, 59%; (iii) Acetic anhydride, pyridine, N₂ atmosphere, RT, overnight, 66%; (iv) 80% aqueous acetic acid, 50 °C, 4 h, 81%; (v) 4-nitrophenyl chloroformate,pyridine, dry DCM, N₂ atmosphere, RT, 4 h; (vi) TEA, THF, N₂ atmosphere, RT, 72 h, 14%.

(i) Diethanol amine, DMSO, reflux 140 °C, 24 h, 69%; (ii) MsCl, pyridine, N₂ atmosphere, 0°C, 0.5 h then reflux 80° C 1 h, 59%; (iii) RaNi, hydrazine monohydrate, DCM/MeOH, RT, 2.5 h; (iv) dry HCl in ether, DCM, 68%; (v) TEA, DMF, N₂ atmosphere, RT, 72 h, 45% and 50%.

Scheme 3. a,b. Synthesis of TCO-N-mustard and TCO-doxorubicin prodrugs.

acid derivative 12 in 66 % yield. Selective deprotection of the O-silyl group at position 9 was performed in aqueous acetic acid to yield the tetra-O-acetyl-protected sialic acid derivative 13 that bears a free hydroxyl group at position 9, in 81 %. The tetra-O-acetyl-9-hydroxy-Neu5Ac methyl ester 13 was then reacted with 4-nitrophenyl chloroformate to insert a good leaving group at position 9 and the 4-nitrophenol derivative 14 was immediately reacted with the Tz-NH $_2$ derivative 15 to yield the Ac $_4$ SiaTz 16 in 14 %.

To prepare the second component of the bioorthogonal reaction (i.e. the prodrugs), two TCO-modified prodrugs, TCO-N-mustard **22** and TCO-doxorubicin **24** were synthesized (Scheme 3a and b). The TCO-prodrugs were purified by column chromatography and characterized using 1H and ^{13}C NMR spectroscopy, and mass spectrometry.

The *N*,*N*-bis-(2-chloroethyl) benzene-1,4-diamine HCl salt **20** was prepared according to our previously reported procedures [22], then it was reacted with the TCO-4-nitrophenyl carbonate **21** in the presence of TEA and DMF to give the TCO-*N*-mustard prodrug **22** in 45 % yield. The same procedure was carried out with the doxorubicin.HCl **23** to give the TCO-doxorubicin prodrug **24** in 50 % yield [23].

2.2. In vitro Tz expression using MGE

To quantify the Tz expression, and determine the selectivity of Tz expression on MCF-7 breast cancer cancerous cells *versus* L929 fibroblast cells (non-cancerous cells with known high metabolic rate) [40,41], western blotting analysis and confocal microscopy imaging were performed. First, the toxicities of the three synthesized Tz-modified monosaccharides, Ac₄ManNTz 7, Ac₄GalNTz 8, and Ac₄SiaTz 16 were determined on both MCF-7 cells and L929 fibroblasts (Table 1) to determine the tolerated concentration for subsequent use for MGE leading to Tz expression. The IC₅₀ values for Ac₄ManNTz 7 and Ac₄GalNTz 8 were found to be 71.27 \pm 0.7 μ M and 71.32 \pm 0.9 μ M, respectively on MCF-7 cells (Table 1). The concentration of monosaccharides typically utilized for MGE applications is 50 μ M [42,43].

Table 1 IC₅₀ values (μ M) for compounds 7, 8, and 16 in the MCF-7 and L929 cells using the MTT assay. Data represented as mean \pm SEM (n = 3).

Compound	IC ₅₀ (μM)	
' <u> </u>	MCF-7	L929
Ac ₄ ManNTz 7	71.2 ± 0.7	99.9 ± 1.5
Ac ₄ GalNTz 8	71.3 ± 0.9	95.9 ± 3.8
Ac ₄ SiaTz 16	97.0 ± 2.7	>120

However, in this study, the concentrations of 10 μ M and 20 μ M were selected as they showed similar cell viability to that obtained with the control in the cell lines selected (in all cases cell viability > 85 %).

Then, since the hypothesis for activation of the TCO-prodrugs at the tumour relies on selective expression of the Tz activator within cancer cell surface glycans, the selectivity of Tz incorporation and expression on breast cancer cells and non-cancerous cells was assessed. MCF-7 cells and L929 fibroblasts were incubated with 10 and 20 μM Ac $_4 ManNTz$ 7, Ac $_4 GalNTz$ 8, and Ac $_4 SiaTz$ 16 for 72 h and Tz expression was determined by Western blotting (Fig. 3). The results showed that 1) the three Tz-modified monosaccharides can cause Tz expression within the MCF-7 breast cancer cells' glycoproteins, 2) Tz expression is proven to be in a concentration-dependant manner (20 μM treatment shows more Tz expression than 10 μM treatment), and 3) the Ac $_4 ManNTz$ 7 and Ac $_4 GalNTz$ 8 derivatives allow more Tz expression compared to the Ac $_4 SiaTz$ 16.

Importantly, with regards to the selectivity of prodrug activation, treatment with 10 or 20 μM concentrations of the three Tz-modified monosaccharides did not lead to any Tz expression in the L929 fibroblasts which suggests that these Tz-modified monosaccharides are more selectively incorporated on breast cancer cells compared to fibroblasts.

To further confirm the Western blotting findings and to quantify the level of Tz expression on the cells, confocal microscopy imaging was

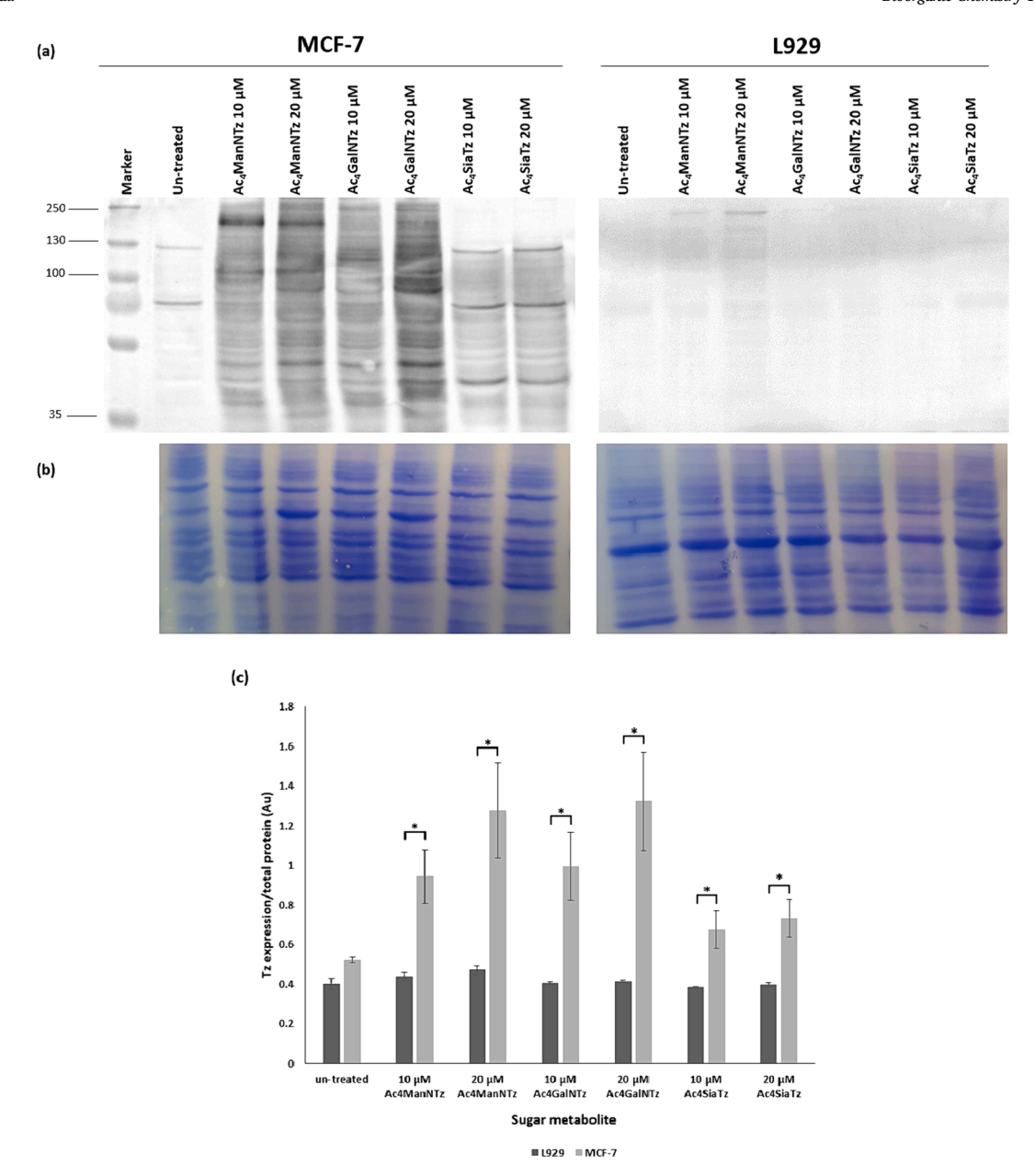


Fig. 3. In vitro selective Tz expression within glycoproteins in MCF-7 cells vs L929 cells. (a) Western blot analysis of Tz reporters on MCF-7 and L929 cells treated separately with the three Tz-modified monosaccharides $Ac_4ManNTz$ 7, $Ac_4GalNTz$ 8, and Ac_4SiaTz 16 (10 and 20 μ M). (b) Total protein loading shown by Coomassie staining. (c) Quantification of Tz expression level compared to total protein in MCF-7 and L929 cells of three independent experiments. Data are presented as mean \pm SEM (n = 3). (*p < 0.05).

carried out to visualize and measure the relative mean fluorescence intensity (MFI). Thus, MCF-7 and L929 cells were incubated with 10 and 20 μ M Ac₄ManNTz **7**, Ac₄GalNTz **8**, and Ac₄SiaTz **16** for 72 h, and then treated with TCO-CY5 dye (Fig. 4a). The results showed the same pattern previously indicated by Western blotting where the three Tzmonosaccharides facilitated Tz expression and hence fluorescence in MCF-7 cells, with the 20 μ M concentration showing more Tz expression than the 10 μ M (almost 1.5 folds higher). In contrast, the L929 cells that were treated with the Tz-modified monosaccharides did not show any significant fluorescence. MFI quantification showed that the 20 μ M concentration of Ac₄ManNTz **7** caused the highest Tz expression in MCF-7 cells among the tested samples and all the three Tz-modified monosaccharides in both tested concentrations (10 μ M and 20 μ M) are selective towards the MCF-7 cells over the L929 fibroblasts (Fig. 4b).

2.3. In vitro prodrug activation

Given the aforementioned feasibility of the three Tz-modified monosaccharides Ac₄ManNTz 7, Ac₄GalNTz 8 and Ac₄SiaTz 16, to induce Tz expression on MCF-7 cells at 10 and 20 μ M concentrations and their selectivity for MCF-7 cells, *in vitro* activation of the TCO-*N*-mustard 22 and TCO-doxorubicin 24 prodrugs by the Tz bioorthogonal ligation reaction was tested in the Tz-engineered MCF-7 cells using the MTT assay (Table 2).

The IC₅₀ of the TCO-doxorubicin prodrug **24** was tested on MCF-7 cells (without pre-treatment with any Tz-modified monosaccharide to act as a control experiment for the prodrug activation) and was found to be 2.5 μ M (>9-fold decrease in parent doxorubicin **23** potency) (IC₅₀ of the parent doxorubicin **23** was found to be 0.3 \pm 0.003 μ M which corresponds to the previously reported value on MCF-7 cells [44–46]). This demonstrates the ability of TCO to mask doxorubicin's activity. For the

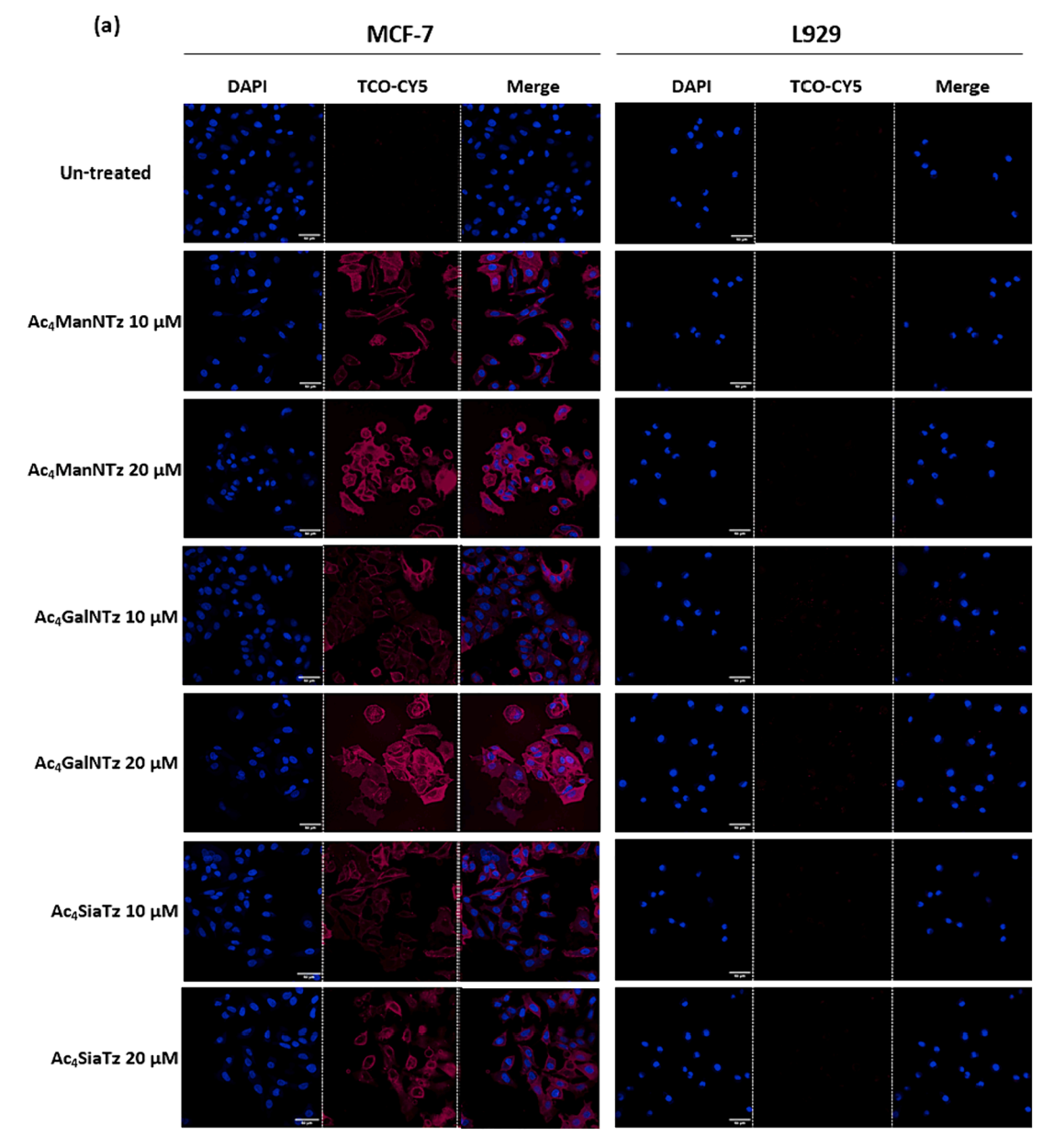


Fig. 4. In vitro Tz expression in MCF-7 and L929 cells. (a) Images representing confocal fluorescence microscopy imaging of Ac₄ManNTz 7, Ac₄GalNTz 8, and Ac₄SiaTz 16-treated MCF-7 and L929 cells (10 and 20 μ M for 72 h). Tz expression was reacted with TCO-Cy5 (20 μ M) for 20 min to visualize the expression (red colour). Scale bar indicates 50 μ m. (b) MFI quantification from Ac₄ManNTz 7, Ac₄GalNTz 8, and Ac₄SiaTz 16-treated MCF-7 and L929 cells of three independent experiments using ImageJ software. Data are presented as mean \pm SEM (n = 3). (*** p < 0.001, **** p < 0.0001).

prodrug activation assessment, MCF-7 cells were first incubated with 10 and 20 μ M of Ac₄ManNTz 7, Ac₄GalNTz 8, and Ac₄SiaTz 16 to allow Tz expression, followed by cells treatment with the TCO-doxorubicin prodrug 24. The IC₅₀ values (Table 2, Fig. 5, and Figure S1 a, b, and c) show recovery of the active doxorubicin's IC₅₀ in a concentration-dependent manner, aligned with the Tz expression patterns previously seen by Western blotting and confocal microscopy imaging. The 20 μ M pre-treatment with the Tz-modified monosaccharides resulted in more prodrug activation and the Ac₄ManNTz 7 and Ac₄GalNTz 8 pretreatment induced more prodrug activation compared to the Ac₄SiaTz 16.

With the TCO-N-mustard prodrug **22**, the IC $_{50}$ of only the prodrug was assessed due to the instability of the active N-mustard drug. The TCO-N-mustard prodrug **22** IC $_{50}$ was found to be 23 μ M on MCF-7 cells and its activation on pre-treated cells with 10 and 20 μ M of Ac $_4$ ManNTz **7**, Ac $_4$ GalNTz **8** and Ac $_4$ SiaTz **16** was also found to be concentration-

dependant (Table 2, Fig. 5, and Figure S1d, e, and f).

To further evaluate the prodrugs' safety on non-cancerous cells, the IC50 values of the TCO-N-mustard prodrug 22 and the TCO-doxorubicin prodrug 24 were assessed on L929 cells ($38\pm0.5~\mu M$ and $6.4\pm0.1~\mu M$, respectively). IC50 values were also measured in these cells after pretreatment with 10 and 20 μM of the three Tz-modified monosaccharides 7, 8, and 16 to test the possibility of any undesirable prodrug activation in non-cancerous cells (prodrug activation would result in a lower IC50). No prodrug activation was generally detected for the $10~\mu M$ pre-treatment. Some activation was observed with the $20~\mu M$ pretreatment with Ac4ManNTz 7 and Ac4GalNTz 8. However, this was relatively small. For example, the IC50 values of the TCO-N-mustard prodrug 22 after the $20~\mu M$ pre-treatment with Ac4ManNTz 7 and Ac4GalNTz 8 were very similar (>72~%) to those observed in the absence of the activator (Table 2, Fig. 5, and Figure S2a-f). These findings prove

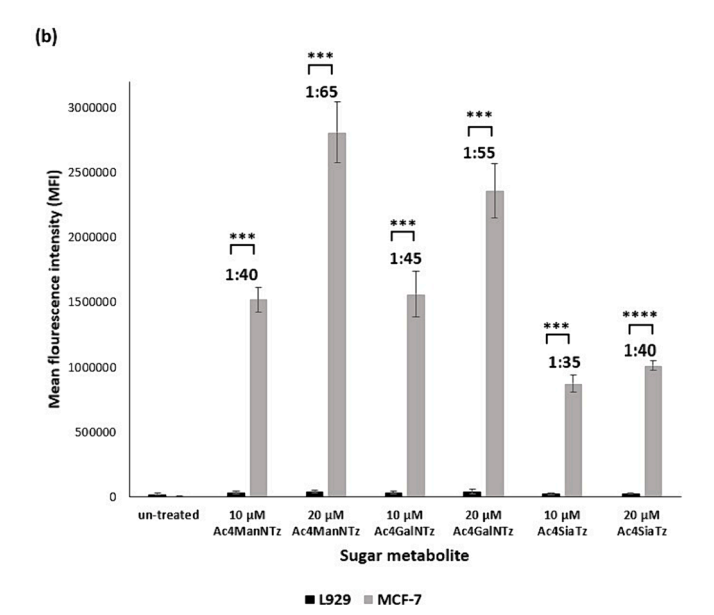


Fig. 4. (continued).

Table 2 IC_{50} values (μM) for compounds 22 and 23 activation in the MCF-7 and L929 cells using the MTT assay. Data represented as mean \pm SEM (n=3).

Compound	IC ₅₀ (μM)	
	MCF-7	L929
Doxorubicin 23 on non-engineered cells	0.3 ±	$2.0 \pm$
	0.03	0.01
TCO-DOX prodrug 24 on non-engineered cells	2.5 \pm	6.4 ± 0.1
	0.03	
TCO-DOX prodrug 24 on 10 μM Ac ₄ ManNTz-engineered cells	0.8 ± 0.1	5.3 ± 0.7
TCO-DOX prodrug 24 on 20 μM Ac ₄ ManNTz-engineered	0.3 \pm	$\textbf{4.2} \pm \textbf{0.3}$
cells	0.02	
TCO-DOX prodrug ${f 24}$ on 10 μM Ac ₄ GalNTz-engineered cells	1.2 ± 0.5	6.0 ± 0.3
TCO-DOX prodrug 24 on 20 μM Ac ₄ GalNTz-engineered cells	0.4 ± 0.1	4.4 ± 0.3
TCO-DOX prodrug 24 on 10 μM Ac ₄ SiaTz-engineered cells	1.8 ± 0.5	6.1 ± 0.6
TCO-DOX prodrug 24 on 20 μM Ac ₄ SiaTz-engineered cells	$\textbf{0.7} \pm \textbf{0.2}$	5.9 ± 0.1
TCO-N-mustard prodrug 22 on non-engineered cells	23.1 \pm	38.0 \pm
	0.6	0.5
TCO-N-mustard prodrug 22 on 10 μM Ac ₄ ManNTz-	$\textbf{4.2} \pm \textbf{0.3}$	28.9 \pm
engineered cells		1.4
TCO-N-mustard prodrug 22 on 20 μM Ac ₄ ManNTz-	2.7 ± 0.3	27.6 \pm
engineered cells		0.9
TCO-N-mustard prodrug 22 on 10 μM Ac ₄ GalNTz-	5.4 ± 0.2	$33.9 \pm$
engineered cells		0.9
TCO-N-mustard prodrug 22 on 20 μM Ac ₄ GalNTz- engineered cells	2.6 ± 0.4	29.7 ± 1.3
TCO-N-mustard prodrug 22 on 10 μM Ac ₄ SiaTz-	6.0 ± 0.7	37.4 ±
engineered cells	• • •	0.1
TCO-N-mustard prodrug 22 on 20 µM Ac ₄ SiaTz-	3.1 ± 0.4	36.0 ±
engineered cells		0.9

the validity of the hypothesis presented in this paper and demonstrate the selectivity of Tz expression and thereby selective prodrug activation in MCF-7 cells over non-cancerous L929 cells.

2.4. Tz presentation selectivity on microglial cells

The brain is a well-known site for breast cancer metastasis, indeed breast cancer is the second most reported cancer type to metastasize to the brain [47–49]. Therefore there is considerable interest in determining selective methods for targeting tumours that have metastasised to the brain, without causing toxicity to non-cancerous brain cells.

Microglial cells are a particularly relevant cell type because they present metabolic similarities to cancer cells (i.e. metabolic rate and PSA expression) [50-53]. Hence the next step of our approach sought to determine whether BV2 microglial cells would express the Tz upon exposure to the Tz-modified monosaccharides. If no Tz expression occured, this would provide preliminary proof of concept results for the cytotoxicity towards breast cancer cells in the presence of non-cancerous brain cells. Ac₄ManNTz 7 which had been found to be the most effective Tz-modified monosaccharide for Tz expression was selected to test this hypothesis. The uptake was also tested for tetra-O-acetyl azidomannosamine (Ac₄ManNAz) which is widely reported to be used for MGE and azide expression [21,43,54], and we had previously demonstrated it to be much less selective between breast cancer cells and noncancerous cells [22]. Confocal microscopy imaging of Ac₄ManNTz 7and Ac₄ManNAz-treated BV2 microglial cells showed no Tz expression, while it showed azide expression within the microglial cell membrane glycans indicating the selectivity of the Tz-modified monosaccharides uptake and incorporation in the cells' surface glycans (Figure s3).

2.5. Serum stability of Tz-modified monosaccharides and TCO-prodrugs

One of the challenges of using compounds bearing the Tz functional group is their reported limited in vivo stability and plasma protein binding [23,55,56]. To determine whether this would also be a limiting factor for our approach, the serum stability of the three Tz-modified monosaccharides 7, 8, and 16 was tested. 7, 8, and 16 were incubated with mouse serum at 37 °C and the amount of the Tz that remained intact was determined by HPLC at $\lambda = 520$ nm (the Tz absorbance maximum which is responsible for its purple colour) [23,57]. Ac₄SiaTz 16 showed the best serum stability among the three compounds with 83 \pm 2.7 % remaining intact after 4 h of serum incubation while Ac₄GalNTz **8** showed 73 \pm 0.9 % remaining intact (p < 0.05) and Ac₄ManNTz **7** was the least stable with 61 \pm 2.2 % remaining intact (p < 0.001) (Fig. 6a). These results align with the serum stability of other previously reported Tz compounds for the same time profile [23,25,58], further supporting the reliability of our Tz-modified monosaccharides. Serum stability for the TCO-prodrugs was also tested by the same experimental method. The TCO-N-mustard 22 prodrug showed very good serum stability at all timepoints with 73 \pm 2.5 % remaining intact after 12 h of serum incubation (Fig. 6b). The TCO-DOX prodrug 24 was stable for a shorter time $(67 \pm 0.7 \% \text{ was intact after 2 h of serum incubation but less than 5 \% at}$ 6 h). However, it should be noted that doxorubicin itself is reported to

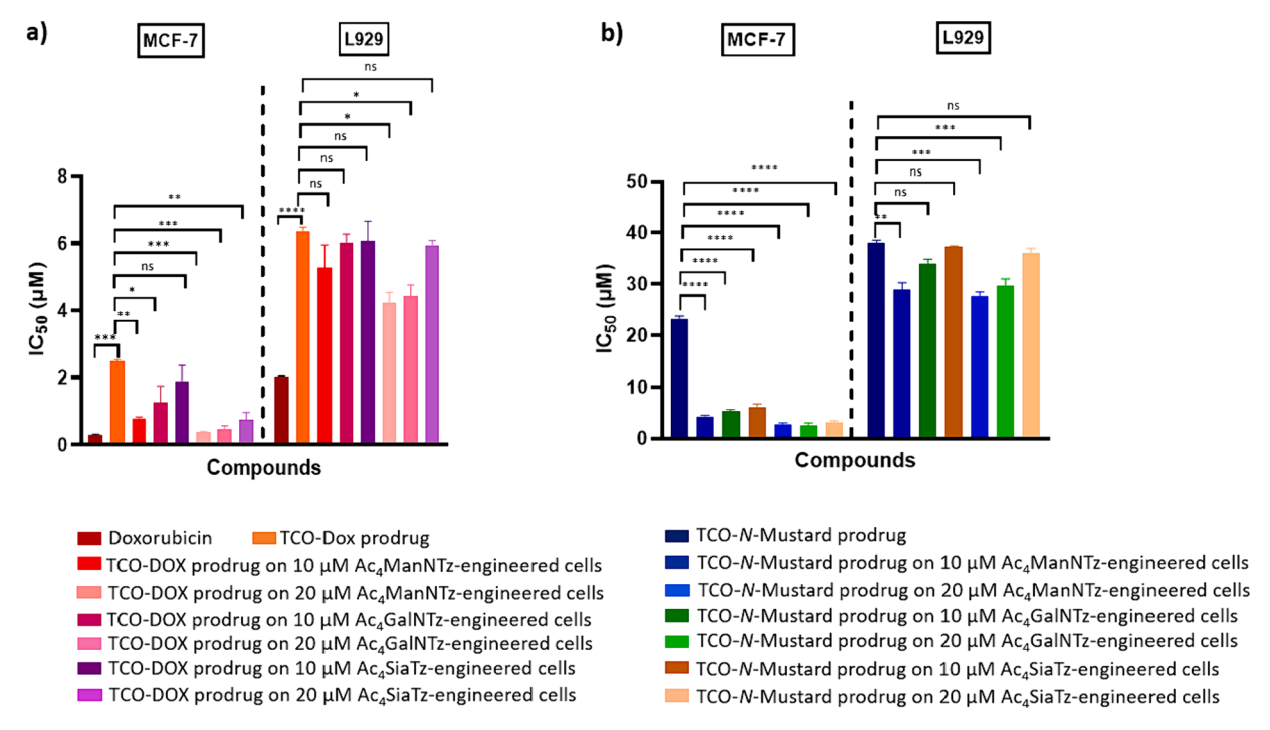


Fig. 5. Statistical significance of the TCO-prodrugs IC_{50} values on non-Tz engineered and Tz-engineered MCF-7 and L929 cells (a) Determined IC_{50} of Doxorubicin 23 and its TCO-prodrug 24 in MCF-7 and L929 cells and the IC_{50} of the TCO-prodrug 24 against 7, 8 and 16 (10 and 20 μM)-engineered MCF-7 and L929 cells. (b) Determined IC_{50} of TCO-*N*-mustard prodrug 22 in MCF-7 and L929 cells and the IC_{50} of the TCO-prodrug 22 against 7, 8, and 16 (10 and 20 μM)-engineered MCF-7 and L929 cells. Data are presented as mean \pm SEM (n = 3). ns p > 0.05, *p < 0.05, *p < 0.05, *p < 0.001, **** p < 0.001 and ***** p < 0.0001.

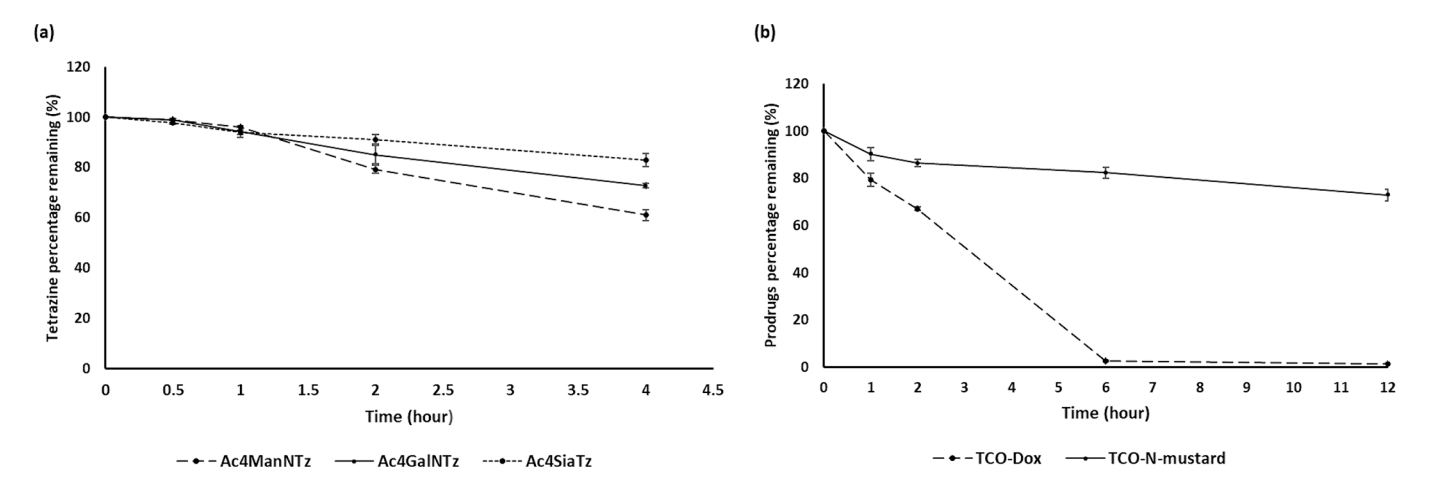


Fig. 6. Serum stability profile of (a) Tz-modified monosaccharides Ac₄ManNTz 7, Ac₄GalNTz 8, and Ac₄SiaTz 16 and (b) TCO-prodrugs TCO-*N*-mustard 22 and TCO-doxorubicin 24 in 50 % mouse serum/PBS at 37 °C monitored by HPLC at $\lambda = 520$ and 233 nm. Data represented as mean \pm SEM (n = 3).

have high plasma protein binding (up to 70 % in 10 min) [59], which suggests that conjugating doxorubicin to the TCO moiety prolongs its stability in serum.

3. Conclusion

This paper elucidates the selective Tz expression within MCF-7 breast cancer cell surface glycans using Tz-modified monosaccharides, and probes the effectiveness of the expressed Tz moieties for activation of TCO-prodrugs. Three novel Tz-modified monosaccharides (Ac₄ManNTz 7, Ac₄GalNTz 8, and Ac₄SiaTz 16) were developed for engineering the Tz moiety on MCF-7 breast cancer cells \emph{via} MGE using relatively low concentrations of the substrates (10 and 20 μ M). Selective Tz expression on MCF-7 breast cancer cells over the non-cancerous L929 (\geq 35 folds higher) was confirmed by Western blot analysis and confocal

microscopy imaging indicating the selective tumour targeting approach. Furthermore, two TCO-prodrugs were developed, specifically a novel TCO-N-mustard prodrug along with a TCO-doxorubicin prodrug. The engineered Tz activators were shown to efficiently mediate the tetrazine ligation reaction *in vitro* and induce the release of parent drugs from the TCO-prodrugs. The level of the Tz expression was shown to affect the extent of the prodrug activation where the Ac₄ManNTz 7 and Ac₄GalNTz 8 derivatives (20 μ M) showed the highest Tz expression leading to full restoration of the activity of the parent cytotoxic drugs. To extend the strategy and further test the selective Tz expression on other types of non-cancerous, highly metabolic cells, Ac₄ManNTz 7 (20 μ M) which showed the highest Tz expression level in MCF-7 cells was shown to not cause Tz expression on BV2 microglial cells. Taken together, these data support the hypothesis of using Tz-modified monosaccharides for selective and concentration-dependent labelling of MCF-7 breast cancer

cells allowing a high degree of selectivity and quantitative control over drug release. Moreover, this study provides theoretical and experimental support for designing bioorthogonal-based prodrug activation systems that can benefit from the MGE concept, especially for breast cancer-targeted chemotherapy. Future studies will therefore focus on determining the toxicity profiles and pharmacokinetic properties of the components reported herein, *in vivo*.

4. Material and method

4.1. Chemistry materials

All chemicals were purchased from Sigma Aldrich, UK. except for the 2-(4-(6-methyl-1,2,4,5-tetrazin-3-yl)phenyl)acetic acid and the (4-(6-methyl-1,2,4,5-tetrazin-3-yl)phenyl)methanamine HCl which were purchased from BLD pharm, Germany. Silica gel pore size 60A (230–400 mesh size and 40–63 μ m particle size) was used for column chromatography. Deuterium oxide (D₂O), or deuterated chloroform (CDCl₃), or deuterated DMSO (DMSO- d_6), or deuterated methanol (CD₃OD) were used as specified per compounds for $^1{\rm H}$ NMR and $^{13}{\rm C}$ NMR.

4.2. Synthesis

Scheme 1.

2,5-Dioxopyrrolidin-1-yl 2-(4-(6-methyl-1,2,4,5-tetrazin-3-yl) phenyl)acetate (2) 2-(4-(6-Methyl-1,2,4,5-tetrazin-3-yl)phenyl)acetic acid 1 (46 mg, 0.2 mmol, 1 eq.) and N-hydroxysuccinimide (23 mg, 0.2 mmol, 1 eq.) were dissolved in anhydrous chloroform (10 mL), then N, N'-diisopropylcarbodiimide DIC (41.2 mg, 0.2 mmol, 1 eq.) was added under N2 atmosphere. The reaction mixture was stirred at room temperature for 4 h. The solvent was removed under vacuum and the residue was purified by column chromatography (hexane: ethyl acetate = 4:1) to yield methyltetrazine-NHS 2 as dark purple crystals (42 mg, 70 %). ¹H NMR (CDCl₃, 400 MHz) δ 2.86 (4H, s, succinimide CH₂-CH₂), 3.11 (3H, s, tetrazine CH₃), 4.06 (2H, s, CH₂COO), 7.59 (2H, d, J = 8.4 Hz, ArH), 8.61 (2H, d, $\overline{J} = 8.4$ Hz, ArH). ¹³C NMR (CDCl₃, 100 MHz) δ 23.51 (CH₃), 25.60 (succinimide CH₂), 37.61 (succinimide CH₂), 42.25 (CH₂), 128.41, 130.27, 131.42, 136.03, 156.81 (CO), 163.78 (Tz ring C), $\overline{166.20}$ (CO), 167.36 (Tz ring C), 168.87 (CO). m/z (FTMS + ESI) M + 1 $(C_{15}H_{14}N_5O_4)$ requires 328.1040 Found 328.1044.

General procedure for the synthesis of ManNTz 5 and GalNTz 6 intermediates. Methyltetrazine-NHS 2 (10 mg, 0.03 mmol, 1 eq.) was dissolved in dry methanol (5 mL), then distance or distance or distance (22 mg, 0.12 mmol, 4 eq.) and TEA (26 μ L) were added. The reaction was sonicated at 50 °C for 30 min until complete dissolution, then the reaction mixture was stirred at room temperature overnight. The solvent was concentrated under vacuum and the residue was then purified by column chromatography (DCM/methanol, 20:1—10:1) to afford the target Tz-modified monosaccharide.

2-(4-(6-Methyl-1,2,4,5-tetrazin-3-yl)phenyl)-2,4,5-trihydroxy-6-(hydroxymethyl)tetrahydro-2*H*-**pyran-3-yl)acetamide** (ManNTz) (5) Following the general procedure, ManNTz 5 was isolated as a dark purple oil (5.2 mg, 44 %). ¹H NMR (D₂O, 400 MHz) δ 2.60 (2H, d, J = 9.9 Hz, C<u>H₂</u>), 2.99 (3H, s, C<u>H₃</u>), 3.46 (1H, t, J = 9.8 Hz, H₅), 3.58 (1H, t, J = 9.6 Hz, H₆), 3.74–3.81 (2H, m, H₆,H₄), 4.00 (1H, dd, J = 3, 4.4 Hz, H₂), 4.28 (1H, dd, J = 3, 9.5 Hz, H₃), 4.41 (1H, d, J = 4.4 Hz, H₁), 5.01 (1H, s, NH), 7.52 (2H, d, J = 8.4 Hz, ArH), 8.32 (2H, d, J = 8.4 Hz, ArH). ¹³C NMR (CD₃OD, 100 MHz) δ 19.65 (<u>C</u>H₃), 42.00 (<u>C</u>H₂), 53.97, 60.91, 67.18, 69.16, 72.09, 93.48, 127.47, 129.83, 130.61, 140.72, 163.88 (Tz ring C), 167.32 (Tz ring C), 172.46 (NH<u>C</u>O). m/z (FTMS + ESI) (M + Na)⁺(C₁₇H₂₁N₅O₆Na) requires 414.1384 Found 414.1378.

2-(4-(6-Methyl-1,2,4,5-tetrazin-3-yl)phenyl)-2,4,5-trihydroxy-6-(hydroxymethyl)tetrahydro-2*H*-pyran-3-yl)acetamide (GalNTz) (6) Following the general procedure, GalNTz 6 was isolated as a dark purple oil (6 mg, 50 %). 1 H NMR (CD₃OD, 400 MHz) δ 3.05 (3H, s, tetrazine C<u>H₃</u>), 3.70–3.78 (4H, m, tetrazine C<u>H₂</u>, H₅, H₆), 3.88 (11*H*, dd,

J=1.5, 9.6 Hz, H₆), 3.93 (1H, dd, J=10.1, 3.2 Hz, H₄), 4.07 (1H, dd, J=3.6, 6.1 Hz, H₂), 4.27 (1H, dd, J=6.1, 10.1 Hz, H₃), 4.61 (1H, s, NH), 5.17 (1H, d, J=3.6 Hz, H₁), 7.62 (2H, d, J=8.4 Hz, ArH), 8.51 (2H, d, J=8.4 Hz, ArH). ¹³C NMR (CD₃OD, 100 MHz) δ 19.64 (<u>C</u>H₃), 42.23 (<u>C</u>H₂), 50.81, 61.37, 68.22, 69.16, 70.26, 91.39, 127.49, 129.83, 130.62, 140.73, 163.88 (Tz ring C), 167.32 (Tz ring C), 172.47 (NH<u>C</u>O). m/z (FTMS + ESI) (M + Na)⁺(C₁₇H₂₁N₅O₆Na) requires 414.1384 Found 414.1384.

General procedure for synthesis of $Ac_4ManNTz$ 7 and $Ac_4GalNTz$ 8. In pyridine (1 mL), ManNTz 5 or GalNTz 6 (5.2 mg, 0.013 mmol) were dissolved. Acetic anhydride (0.5 mL) was added gradually under N_2 atmosphere to the solution at 0 °C. The reaction mixture was left to warm to room temperature and stirred overnight. The pyridine was coremoved with toluene under vacuum then the residue was dissolved in DCM and washed with 1 M HCl, brine, and water, dried over anhydrous Na_2SO_4 , filtered and concentrated under vacuum. The residue was purified by column chromatography (hexane/ethyl acetate, 2:1—1:1) to afford the target acetylated Tz-modified monosaccharide.

6-(Acetoxymethyl)-3-(2-(4-(6-methyl-1,2,4,5-tetrazin-3-yl) phenyl)acetamido)tetrahydro-2H-pyran-2,4,5-triyl (Ac₄ManNTz) (7) Following the general procedure, Ac₄ManNTz 7 was isolated as a dark purple oil (5 mg, 67 %). ¹H NMR (CDCl₃, 400 MHz) δ 1.94-2.07 (9H, m, OAc), 2.17 (3H, s, OAc), 3.11 (3H, s, tetrazine CH₃), 3.76 (2H, d, J = 9.9 Hz, tetrazine CH₂), 3.93-4.06 (2H, m, H₅, H₆), 4.20(1H, dt, J = 12.6, 4.8 Hz, H₆), 4.68 (1H, dd, J = 8.3, 5.1 Hz, H₂), 5.07 $(1H, dd, J = 10.2, 8.6 Hz, H_4), 5.31 (1H, dd, J = 10.2, 5.1 Hz, H_3), 5.80$ $(1H, s, H_1), 6.00 (1H, s, NH), 7.55 (2H, d, J = 7.3 Hz, ArH), 8.62 (2H, d, H_1), 8.62 (2H, d, H_2)$ J = 7.4 Hz, ArH). ¹³C NMR (CDCl₃, 100 MHz) δ 14.21 (<u>C</u>H₃), 20.60 (COCH₃), 20.65 (COCH₃), 20.85 (COCH₃), 21.19 (COCH₃), 43.52 (CH₂), 49.50, 60.41, 61.81, 65.09, 69.02, 70.10, 91.51, 128.44, 128.58, 130.08, 130.15, 131.12, 139.09, 168.10, 169.45, 169.95, 170.13, 170.41 (NHCO). m/z (FTMS + ESI) (M + Na)⁺(C₂₅H₂₉N₅O₁₀Na) requires 582.1807 Found 582.1795. HPLC analysis: MeCN - H₂0 (20:80-70:30), 96.61 % purity.

6-(Acetoxymethyl)-3-(2-(4-(6-methyl-1,2,4,5-tetrazin-3-yl) phenyl)acetamido)tetrahydro-2H-pyran-2,4,5-triyl triacetate (Ac4GalNTz) (8) Following the general procedure, Ac4GalNTz 8 was isolated as a dark purple oil (6.3 mg, 74 %). 1 H NMR (CDCl₃, 400 MHz) δ 1.93 (3H, s, OAc), 2.02 (6H, m, OAc), 2.16 (3H, s, OAc), 3.11 (3H, s, tetrazine CH_3), 3.63 (2H, d, J = 4.0 Hz, tetrazine CH_2), 3.99–4.12 (2H, m, H_5 , H_6), 4.18 (1H, t, J = 6.9 Hz, H_6), 4.65–4.74 (1H, m, H_2), 5.13 (1H, dd, J = 11.5, 3.2 Hz, H₄), 5.36–5.41 (2H, m, H₃ H₁), 6.23 (1H, s, NH), 7.44 (2H, d, J = 8.3 Hz, ArH), 8.57 (2H, dd, J = 8.3, 3.7 Hz, ArH). ¹³C **NMR** (CDCl₃, 100 MHz) δ 20.52 (CH₃), 20.64 (COCH₃), 20.69 (COCH₃), 20.81 (COCH₃), 21.20 (COCH₃), 43.65 (CH₂), 47.30, 61.23, 66.61, 67.65, 67.68, 68.66, 91.00, 128.55, 130.12, 131.18, 139.05, 167.46, 168.61, 170.09, 170.36, 171.06 (NHCO). m/z (FTMS + ESI) (M + Na)⁺(C₂₅H₂₉N₅O₁₀Na) requires 582.1807 Found 582.1810. **HPLC** analysis: MeCN - H₂0 (20:80-70:30), 100 % purity.

Scheme 2.

5-Acetamido-3,5-dideoxy-D-glycero-D-galacto-2-nonulosonic acid methyl ester (10) Synthesis of compound 10 was proceeded as previously reported[22] "N-Acetylneuraminic acid 9 (1.00 g, 3.23 mmol, 1 eq.) was dissolved in dry methanol (20 mL) followed by the addition of trifluoroacetic acid (0.07 mL, 11.64 mmol, 3.6 eq.). The mixture was stirred until clear solution was obtained. The solvent was removed under vacuum and white solid of Neu5Ac methyl ester 10 was obtained and used without further purification (0.9 g, 86 %); $[\alpha]_D^{20}$ -18 (c 1.0, MeOH), lit [60]. -31.7 (c 1.0, H₂O); m.p. 182-184C°, lit [61]. 182–184 °C. ¹H NMR (D₂O, 400 MHz) δ 1.82 (1H, dd, J = 12.0, 13.0 Hz, H_3), 1.95 (3H, s, NHCOC H_3), 2.22 (1H, dd, J = 5.0, 13.0 Hz, H_3), 3.45 (1H, dd, J = 5.0, 9.0 Hz, H₇), 3.52 (1H, dd, J = 6.5, 12.0 Hz, H₉·), 3.63 (1H, ddd, J = 2.5, 6.4 Hz, J = 9.0 Hz, H₈), 3.71–3.77 (4H, m, COOCH₃, H_9), 3.83 (1H, t, J = 10.2 Hz, H_5), 3.92–3.99 (2H, m, H_4 , H_6). ¹³C NMR (D₂O, 100 MHz) δ 22.02 (NHCOCH₃), 38.62, 52.02, 53.45 (COOCH₃), 63.11, 66.62, 68.16, 70.06, 70.30, 95.30, 171.37 (NHCOCH₃), 174.80

(COOCH₃)." m/z (FTMS + ESI) (M + Na)⁺(C₁₂H₂₁NO₉Na) requires 346.1109 Found 346.1103.

5-Acetamido-9-O-(tert-butyldimethylsilyl)-3,5-dideoxy-D-glycero-p-galacto-2-nonulosonic acid methyl ester (11) In pyridine, 10 (400 mg, 1.24 mmol, 1 eq.) was dissolved. Then, tert-butyldimethylsilyl chloride TBDMSCl (185 mg, 1.24 mmol, 1 eq.) was added gradually at 0 °C under N₂ atmosphere. The reaction mixture was left to warm to room temperature and stirred overnight. The pyridine was co-removed with toluene under vacuum, then the residue was dissolved in water and extracted by ethyl acetate (3x10 mL). The ethyl acetate was dried over anhydrous Na₂SO₄, filtered, and removed under vacuum to yield 9-O-(tert-butyldimethylsilyl)- Neu5Ac methyl ester 11 as colorless crystals (320 mg, 59 %). ¹H NMR (CD₃OD, 400 MHz) δ 0.00 (6H, s, C(C<u>H</u>₃)₂), 0.83 (9H, s, C(CH₃)₃), 1.80 (1H, dt, J = 13.0, 8.6 Hz, H₃), 1.91 (3H, s, NHCOCH₃), $2.1\overline{3}$ (1H, dd, J = 12.9, 5.0 Hz, H₃), 3.47 (1H, dd, J = 9.3, 1.4 Hz, H₇), 3.60 (1H, ddd, J = 9.2, 4.3, 2.7 Hz, H₈), 3.69 (3H, s, COOCH3), 3.72 (1H, dd, J = 4.5, 1.6 Hz, H₅), 3.74 – 3.79 (1H, m, H₉), $3.89 (\overline{1H}, dd, J = 4.1, 2.7 Hz, H_9), 3.92-4.02 (2H, m, H_4, H_6).$ ¹³C NMR $(CD_3OD, 100 \text{ MHz}) \delta -6.56 (Si(CH_3)_2), -5.02 (Si(CH_3)_2), 13.06, 17.89$ (SiC(CH₃)₃), 21.21 (NHCOCH₃), 24.78 (SiC(CH₃)₃), 25.05 (SiC(CH₃)₃), 39.36, 51.71, 53.09 (COOCH₃), 64.34, 66.30, 67.90, 70.25, 70.74, 95.29, 170.35 (NHCOCH₃), 173.74 (COOCH₃), m/z (FTMS + ESI) (M + Na)⁺(C₁₈H₃₅NO₉SiNa) requires 360.1973 Found 360.1962.

5-Acetamido-9-O-(tert-butyldimethylsilyl)-2,4,7,8-tetra-Oacetyl-3,5-dideoxy-D-glycero-D galacto-2-nonulosonic acid methyl ester (12) 9-O-(tert-Butyldimethylsilyl)- Neu5Ac methyl ester 11 (320 mg, 0.74 mmol, 1 eq.) was dissolved in dry pyridine (1 mL). Then, acetic anhydride (0.5 mL) was added gradually at 0 °C under N2 atmosphere. The reaction mixture was left to warm to room temperature and stirred overnight. The pyridine was co-removed with toluene under vacuum then the residue was dissolved in DCM and washed with 1 M HCl and water, dried over anhydrous Na₂SO₄, filtered, and concentrated under vacuum. The residue was then purified by column chromatography (ethyl acetate) to yield the tetra-O-acetyl-9-O-(tert-butyldimethylsilyl)-Neu5Ac methyl ester 12 as a sticky colorless oil (290 mg, 66 %). ¹H **NMR** (CDCl₃, 400 MHz) δ 0.00 (6H, s, C(CH₃)₂), 0.84 (9H, s, C(CH₃)₃), 1.87 (3H, s, NHCOCH₃), 1.99–2.04 (6H, m, OAc), 2.07 (1H, dd, J = 13.5Hz, H₃), 2.11–2.16 (6H, m, OAc), 2.58 (1H, dd, J = 13.5, 5.0 Hz, H₃), 3.63 (1H, td, J = 11.3, 6.0 Hz, H₉), 3.79 (3H, s, COOCH3), 3.84–3.98 $(2H, m, H_5, H_9), 4.19 (1H, dd, J = 10.7, 2.0 Hz, H_6), 4.95 (1H, td, J = 10.7, 2.0 Hz, H_6)$ 9.0, 6.0, 3.0 Hz, H₈), 5.26–5.47 (2H, m, H₄, H₇). ¹³C NMR (CDCl₃, 100 MHz) $\delta = 5.51 \text{ (Si(CH₃)₂)}, -5.19 \text{ (Si(CH₃)₂)}, 14.20, 18.21 \text{ (SiC(CH₃)₃)},$ 20.78 (COCH₃), 20.87 (COCH₃), 20.97 (COCH₃), 23.23 (NHCOCH₃), 25.74 (SiC(CH₃)₃), 35.82, 49.91, 53.11 (COOCH₃), 60.41, 61.06, 67.94, 68.16, 72.42, 73.11, 97.70, 166.40 (COCH₃), 168.26 (COCH₃), 170.19 (COCH₃), 170.24 (COCH₃), 170.27 (NHCOCH₃), 170.87 (COOCH₃). m/z **(FTMS** + **ESI)** $(M + Na)^{+}(C_{26}H_{43}NO_{13}SiNa)$ requires 628.2396 Found 628.2380.

5-Acetamido-2,4,7,8-tetra-O-acetyl-3,5-dideoxy-D-glycero-D-galacto-2-nonulosonic acid methyl ester (13) Tetra-O-acetyl-9-O-(tertbutyldimethylsilyl)-Neu5Ac methyl ester **12** (435 mg, 0.72 mmol, 1 eq.) was dissolved in 80 % aqueous acetic acid (6 mL) and was stirred at $50\,^{\circ}\text{C}$ for 4 h. The reaction solution was concentrated under vacuum and the residue was purified by column chromatography (petroleum ether: ethyl acetate = 1:1; ethyl acetate: methanol = 95:5) to yield the tetra-Oacetyl-9-hydroxy-Neu5Ac methyl ester 13 as a sticky colorless oil (285 mg, 81 %). ¹H NMR (CDCl₃, 400 MHz) δ 1.90 (3H, s, NHCOCH₃), 2.00-2.25 (12H, m, OAc), 2.54 (1H, dd, J = 13.0 Hz, H₃), 2.64-2.71 (1H, m, H₃), 3.46-3.61 (1H, m, H₉), 3.77 (3H, s, COOCH₃), 3.88-4.03 (1H, m, H_{9}), 4.01–4.11 (1H, m, H_{5}), 4.17–4.31 (1H, m, $\overline{H_{7}}$), 4.82–4.95 (1H, m, H₈), 5.15–5.31 (2H, m, H₄, H₆). 13 C NMR (CDCl₃, 100 MHz) δ 20.79 (COCH₃), 20.87 (COCH₃), 20.97 (COCH₃), 20.98 (COCH₃), 23.16 (NHCOCH₃), 35.90, 49.31, 53.29 (COOCH₃), 60.41, 67.51, 68.25, 72.81, 73.00, 97.62, 166.26 (COCH₃), 168.30 (COCH₃), 169.73 (COCH₃), 170.25 (COCH₃), 171.20 (NHCOCH₃), 171.94 (COOCH₃). m/z **(FTMS** + **ESI)** $(M + Na)^{+}(C_{20}H_{29}NO_{13}Na)$ requires 514.1531 Found

514.1522.

5-Acetamido-9-O-(6-methyl-1,2,4,5-tetrazine-3-benzyl-carbamoyl)-2,4,7,8-tetra-O-acetyl-3,5-dideoxy-D-glycero-D-galacto-2nonulosonic acid methyl ester (16) Tetra-O-acetyl-9-hydroxy-Neu5Ac methyl ester 13 (200 mg, 0.41 mmol, 1 eq.) was dissolved in dry DCM. Then, pyridine (0.14 mL, 1 mmol, 2.5 eq.) was added dropwise at 0 $^{\circ}$ C under N₂ atmosphere, then 4-nitrophenyl chloroformate (123 mg, 0.61 mmol, 2 eq.) was added. The reaction was left to stir at room temperature and protected from light for 4 h. The reaction solution was then added dropwise to a solution of (4-(6-methyl-1,2,4,5-tetrazin-3-yl) phenyl)methanamine HCl (20 mg, 0.08 mmol, 2 eq.) in THF followed by addition of TEA (23 μ L, 0.16 mmol, 4 eq.) and left to stir under N_2 atmosphere and at room temperature for 3 days. The reaction solution was concentrated under vacuum and the residue was purified by column chromatography (petroleum ether: ethyl acetate = 2:1) to yield the Ac₄SiaTz **16** as purple solid (3.1 mg, 14 %). ¹H NMR (CDCl₃, 400 MHz) δ 1.91 (3H, s, NHCOCH₃), 1.97–2.25 (12H, m, OAc), 2.57 (1H, dd, J =13.0, 13.1 Hz, H₃), 3.09 (3H, s, tetrazine CH₃), 3.76 (3H, s, COOCH₃), 4.04-4.19 (2H, m, H₃', H₉), 4.47 (2H, d, J = 5.7 Hz, tetrazine CH₂), 4.65 $(1H, dd, J = 12.2, 8.7 Hz, H_0), 4.95-5.11 (1H, m, H_5), 5.15-5.26 (3H, m, H$ H_6 , H_7 , H_8), 5.32 (1H, dd, J = 13.2, 6.2 Hz, H_4), 7.55 (2H, d, J = 8.4 Hz, ArH), 8.55 (2H, d, J = 8.4 Hz, ArH). ¹³C NMR (CDCl₃, 100 MHz) δ 14.65, 17.49 (CH₃), 20.84 (COCH₃), 23.20 (COCH₃), 23.84 (NHCOCH₃), 29.70 (COCH₃), 31.46 (COCH₃), 36.51, 40.84 (CH₂), 49.01, 52.97 (COOCH₃), 66.69, 67.20, 68.32, 69.63, 73.94, 95.26, 122.04, 125.28, 128.52, 129.03, 145.49, 152.37 (COCH₃), 155.58 (COCH₃), 162.58 (Tz ring C), 168.33 (Tz ring C), 168.65 (COCH₃), 170.03 (COCH₃), 170.30 (NHCOCH₃), 170.41 (NHCOO), 170.89 (COOCH₃). m/z (FTMS + ESI) $(M + Na)^+(C_{31}H_{38}N_6O_{14}Na)$ requires 741.2338 Found 741.2330. **HPLC** analysis: MeCN - H₂0 (20:80-70:30), 96.90 % purity.

Scheme 3.

Compounds **18**, **19**, and **20** were prepared and characterized according to previously reported procedures. [22].

(4-(bis(2-chloroethyl)amino)phenyl) (E)-Cyclooct-2-en-1-yl carbamate (22) (E)-cyclooct-2-en-1-yl (4-nitrophenyl) carbonate 21 (7 mg, 0.024 mmol) was dissolved in DMF (4 mL) under an inert atmosphere. The dihydrochloride salt 20 (6.3 mg, 0.027 mmol) was added with TEA (50 µL, 0.37 mmol) and the reaction mixture was stirred at room temperature for 3 days. The solvent was removed under vacuum and the product was purified using flash column chromatography (hexane/ethyl acetate, 8:1—4:1) to yield the (E)-cyclooct-2-en-1-yl (4-(bis(2-chloroethyl)amino)phenyl)carbamate 22 as a pale yellow oil (4.2 mg, 45 %). ¹H NMR (DMSO- d_6 , 400 MHz) δ 0.70 – 0.92 (1H, m, TCO H_6), 1.12 - 1.22 (1H, m, TCO H_6), 1.44 (1H, dt, J = 12.9, 8.3 Hz, TCO H_7), 1.59 – 1.75 (2H, m, TCO $H_{7'}$, H_5), 1.76 – 1.88 (1H, m, TCO $H_{5'}$), 1.90—2.03 (3H, m, TCO H₈, H₄, H₄), 2.42 (1H, d, J = 10.5 Hz, TCO H_8), 3.61 – 3.75 (8H, m, CH_2 - CH_2 -Cl), 5.28 (1H, s, $TCO H_3$), 5.54 – 5.68 (1H, m, TCO CH = CH), 5.76 (1H, dd, J = 10.5, 8.3 Hz, TCO CH = CH),6.70 (2H, d, J = 8.1 Hz, Ar-H), 7.29 (2H, d, J = 8.0 Hz, Ar-H), 9.29 (1H, s, NH). $^{13}{\rm C}$ NMR (DMSO- d_6 , 100 MHz) δ 24.19, 24.31, 28.86, 35.70, 36.11, 41.72 (CH₂-CH₂-Cl), 52.85 (CH₂-CH₂-Cl), 112.89, 129.92, $129.96, 131.34, \overline{132.66}$ (TCO CH = CH), $153.\overline{35}$ (NHCO). m/z (FTMS + **ESI)** $M^+(C_{19}H_{27}N_2^{35}Cl_2O_2)$ requires 385.1435. Found 385.1444. **HPLC** analysis: MeCN - H₂0 (20:80-70:30), 96.15 % purity.

(*E*)-Cyclooct-2-en-1-yl (3-hydroxy-2-methyl-6-(((1S,4R)-4,5,12-trihydroxy-4-(2-hydroxyacetyl)-10-methoxy-6,11-dioxo-1,2,3,4,6,11-hexahydrotetracen-1-yl)oxy)tetrahydro-2*H*-pyran-4-yl)carbamate (24) (*E*)-Cyclooct-2-en-1-yl (4-nitrophenyl) carbonate 21 (6 mg, 0.0167 mmol) was dissolved in DMF (3 mL) under an inert atmosphere. Doxorubicin 23 (10.9 mg, 0.02 mmol) and TEA (25 μ L, 0.184 mmol) were added and the reaction mixture was stirred in the dark at room temperature for 3 days. The solvent was removed under vacuum and the product was extracted with DCM and washed with sat. NaCO₃ and water. The organic layer was dried over Na₂SO₄ and purified using flash column chromatography (DCM; DCM/Methanol, 95:5) to yield the (*E*)-cyclooct-2-en-1-yl (3-hydroxy-2-methyl-6-(((1S,4R)-4,5,12-

trihydroxy-4-(2-hydroxyacetyl)-10-methoxy-6,11-dioxo-1,2,3,4,6,11hexahydrotetracen-1-yl)oxy)tetrahydro-2H-pyran-4-yl)carbamate 24 as a red fine powder (7.2 mg, 50 %). 1 H NMR (CDCl₃, 400 MHz) δ 0.75 – 0.92 (2H, m, TCO H₆, OH), 1.24 – 1.35 (4H, m, Dox CH₃ sugar ring, TCO H₆'), 1.62—2.05 (7H, m, TCO H₈, H₄, H₄', H₅, H₅', H₇, H₇'), 2.18 (1H, t, J = 14.5 Hz, Dox H₃'), 2.34 (1H, d, J = 14.6 Hz, Dox H₃', 2.40 – 2.46 $(1H, m, TCO H_8), 2.97 (1H, d, J = 12.1 Hz, Dox H_8), 3.05 (1H, d, J = 12.1 Hz, Dox H_8), 3.05 (1H, d, J = 12.1 Hz, Dox H_8)$ 12.1 Hz, Dox Hg/), 3.30 (1H, d, J = 6.2 Hz, Dox H_{10}), 3.69 (1H, d, J = 6.2Hz, Dox H_{10}), 3.88 (1H, s, OH), 4.09 (3H, s, Dox OCH₃), 4.15 (1H, q, J =4.7 Hz, Dox H₆), 4.53 (1H, s, Dox H₄), 4.76 (2H, d, \overline{J} = 4.6 Hz, Dox CO- CH_2 -OH), 5.08 (1H, s, Dox H_5), 5.29 (2H, t, J = 13.8 Hz, TCO H_3 , Dox $\overline{H_7}$, 5.52 (2H, m, TCO CH = CH, Dox $\overline{H_2}$), 5.78 (1H, m, TCO CH = CH), 7.40 (1H, d, J = 8.4 Hz, Dox H₃), 7.80 (1H, t, J = 8.4, 7.4 Hz, Dox H₂), 8.06 (1H, d, J = 7.4 Hz, Dox H₁), 13.28 (1H, s), 14.00 (1H, s). ¹³C NMR $(CDCl_3, 100 \text{ MHz}) \delta 16.86 (CH_3), 24.05, 29.07, 29.66, 34.03, 35.65,$ 35.88, 40.61, 46.79, 56.70 (OCH₃), 65.56, 67.31 (CH₂OH), 69.61, 69.72, 74.12, 100.69, 111.43, 111.64, 118.45, 119.88, 120.93, 131.29, 131.79 (TCO CH = CH), 133.61, 133.66, 135.55, 135.80, 155.01, 155.71, 156.19, 161.08 (NHCOO), 186.75 (CO), 187.17 (CO), 213.90 (COCH₂OH). m/z (FTMS + ESI) (M + Na)⁺ (C₃₆H₄₁NNaO₁₃) requires 718.2470. Found 718.2456. HPLC analysis: MeCN - H₂0 (20:80-70:30), 96.82 % purity.

4.3. Cell culture materials

Human breast adenocarcinoma epithelial cell line (MCF-7) and mouse fibroblasts (L929) were purchased from the American Type Culture Collection (ATCC, Rockville, MD, USA), and BV2 microglial cells were gifted by Dr. Eder, St George's University. Culture media and FBS were purchased from GibcoTM, UK. RIPA buffer, protease inhibitor cocktails and DBCO-CY5 were purchased from Thermo Fisher Scientific, UK. TCO-PEG₄-biotin and TCO-Cy5 were purchased from Tebubio LTD, UK. streptavidin-horseradish peroxidase was purchased from Cell Signalling Technology, UK.

MCF-7 cells were cultured in RPMI-1640 (with added 5 % FBS), mouse fibroblasts L929 and BV2 mouse microglial cells were cultured in DMEM medium (5 g/L and 1 g/L glucose, respectively) (with added 10 % FBS).

4.4. In vitro chemical tags analysis

4.4.1. Western blotting

General procedures were followed as previously reported [22].

MCF-7 and L929 cells were cultured into 6-well plates (at seeding densities of 4×10^4 cell/mL and 1×10^4 cell/mL, respectively). Media supplemented with 10 and 20 μM Ac₄ManNTz, Ac₄GalNTz, and Ac₄SiaTz or with no Tz-modified monosaccharide (control) were added separately to the cells and left to incubate at 37 °C 5 % CO₂ incubator for 72 h. At confluency, cells were prepared for lysation by washing with ice-cold PBS (twice), then, ice-cold RIPA buffer freshly mixed with 1 % protease inhibitor cocktail was added. Cells were scraped and the lysates were centrifuged at 4 °C and supernatants were collected. BCA assay was used to determine the total protein quantity per each sample. For preparation of the western blotting samples, different volumes of lysates containing an equivalence of 20 µg protein were mixed with TCO -PEG₄-biotin (0.5 mM) for 20 min at room temperature. Samples were mixed with loading buffer (4x Laemmli buffer + 10 % β-mercaptoethanol) and heated at 95 °C for 7 min. Samples were then loaded on and separated by 8 % SDS-PAGE gel and the protein bands were transferred onto PVDF membranes. The membranes were blocked with 5 % BSA in 1x TBS-T buffer (50 mM Tris, 150 mM NaCl, 0.1 % Tween20, pH = 7.4) for 1 h at room temperature. Membranes were then incubated with streptavidin-HRP (dilution 1:2000 in TBS-T buffer) at 4 $^{\circ}\text{C}$ for overnight. Then, the membranes were washed trice (15 min) with TBS-T and the protein bands were detected with Pierce™ ECL system.

4.4.2. Confocal microscopy imaging

General procedures were followed as previously reported [22].

MCF-7 and L929 cells were seeded into 35 mm covered glass-bottom confocal dishes (at seeding densities of 4×10^4 cell/mL and 1×10^4 cell/ mL, respectively). Media supplemented with 10 and 20 μ M Ac₄ManNTz, Ac₄GalNTz, and Ac₄SiaTz or with no Tz-modified monosaccharide (control) were added separately to the dishes and left to incubate at 37 °C 5 % CO₂ incubator for 72 h. All media were aspirated from the dishes and cells were washed with DPBS (twice) and then TCO-Cy5containing fresh medium (20 μM) was added to the dishes and left to incubate at 37 $^{\circ}\text{C}$ for 20 min. Medium was aspirated and cells were washed with DPBS (twice) and a 4 % formaldehyde fixative was added at room temperature for 10 min in dark. Fixative was aspirated and cells were washed again with DPBS (twice) and mounted DAPI (1 µL/mL DPBS). Cells were imaged by confocal laser microscope (Nikon A1R Confocal). MFI values (absolute values) were analyzed using ImageJ software and presented as mean \pm SEM. The same protocol was applied with the BV2 microglial cells using Ac₄ManNTz- and Ac₄ManNAz-containing media and TCO-Cy5 or DBCO-Cy5, respectively.

4.5. In vitro prodrug activation

General procedures were followed as previously reported [22].

MCF-7 and L929 cells were incubated with 10 and 20 μM Ac₄ManNTz-, Ac₄GalNTz-, and Ac₄SiaTz-containing RPMI and DMEM media, respectively at 37 °C 5 % CO₂ incubator for 72 h. Cells were then seeded into 96-well plates (at seeding densities of 4×10^4 cell/mL and 1 \times 10⁴ cell/mL for MCF-7 and L929, respectively) and incubated at 37 °C 5 % CO₂ incubator for 24 h. Concentration range of the prodrugs (0.001–10 $\mu M)$ was used to treat the cells and further incubated at 37 $^{\circ} C$ 5 % CO₂ incubator for 67 h. MTT solution (0.5 mg/mL MTT in PBS) was added in each well and further left to incubate at 37 °C 5 % CO2 incubator for 5 h. All treatments-containing media and MTT solution were carefully aspirated from the cells and DMSO (100 µL) was added to dissolve the formed formazan crystals. After incubation for 30 min, the formazan absorbance ($\lambda = 560 \text{ nm}$) was recorded by microplate reader (infiniteF50 TECAN). The assays were performed in three independent replicates. Cells without treatments were used as the control and IC50 values were determined using GraphPad Prism 8.0.2. Data were represented as mean \pm SEM.

4.6. Statistical analysis

Statistical analysis was carried out (for TCO-Dox prodrug **24** or TCO-*N*-mustard prodrug **22** on Ac₄ManNTz-, Ac₄GalNTz-, and Ac₄SiaTz-engineered MCF-7 and L929 cells against the TCO-Dox prodrug **24** or the TCO-*N*-mustard prodrug **22** on non-engineered MCF-7 and L929 cells) by one-way ANOVA followed by Bonferroni's *post hoc* test. Statistical significance was set at p < 0.05 (specifically, ns for non-significant, ** p < 0.01; *** p < 0.001 and **** p < 0.0001).

4.7. Serum stability of Tz-modified monosaccharides and TCO-prodrugs

The stability of Ac₄ManNTz, Ac₄GalNTz, Ac₄SiaTz, TCO-DOX, and TCO-*N*-mustard was evaluated in 50 % mouse serum/PBS over time. Stock solutions of **7**, **8**, **16**, **22**, and **24** (2.4 mM in DMSO) were prepared and then diluted to 1.2 mM in 50 % mouse serum/PBS. After incubation for various time intervals (0, 0.5, 1, 2, and 4 h for the Tz-modified monosaccharides, and 0, 1, 2, 6, and 12 h for the TCO-prodrugs), samples were mixed with 350 μ L of cold acetonitrile for extraction. The samples were then centrifuged (1560 g, 5 min), clear supernatant was collected and analyzed by HPLC. Samples (30 μ L) were injected into HPLC and analyzed by a gradient elution method using an aqueous gradient in acetonitrile (25 min run, 1 mL/min flow, 20 % of acetonitrile increasing to 70 % over 25 min, returning to 20 % for 5 min, UV detection at λ = 520 and 233 nm).

CRediT authorship contribution statement

Madonna M.A. Mitry: Writing – original draft, Methodology, Funding acquisition, Formal analysis, Data curation, Conceptualization. Mark L. Dallas: Writing – review & editing, Methodology, Conceptualization. Samuel Y. Boateng: Writing – review & editing, Methodology, Data curation. Francesca Greco: Writing – review & editing, Supervision, Conceptualization. Helen M.I. Osborn: Writing – review & editing, Supervision, Conceptualization.

Declaration of competing interest

The authors declare that they have no known competing financial interests or personal relationships that could have appeared to influence the work reported in this paper.

Acknowledgements

The authors acknowledge the Egyptian Ministry of Higher Education and Scientific Research, and The British Council (Newton-Mosharafa Fund) represented by the Egyptian Bureau for Cultural and Educational Affairs in London for financial support as well as the University of Reading for provision of the Chemical Analysis Facility. We are also thankful to the PhD student, Nagihan Ozsoy, for supplying and maintaining the BV2 microglial cells.

Appendix A. Supplementary data

Supplementary data to this article can be found online at https://doi.org/10.1016/j.bioorg.2024.107304.

References

- H.B. Ahmed, M.M. Mikhail, A.E.M. Abdallah, M. El-Shahat, H.E. Emam, Pyrimidine-5-carbonitrile derivatives as sprout for CQDs proveniences: Antitumor and anti-inflammatory potentiality, Bioorg. Chem. 141 (2023) 106902, https://doi. org/10.1016/j.bioorg.2023.106902.
- [2] C. Carr, J. Ng, T. Wigmore, The side effects of chemotherapeutic agents, Curr. Anaesth. Crit. Care 19 (2008) 70–79, https://doi.org/10.1016/j.cacc.2008.01.004.
- [3] M. Sheibani, Y. Azizi, M. Shayan, S. Nezamoleslami, F. Eslami, M.H. Farjoo, A. R. Dehpour, Doxorubicin-induced cardiotoxicity: An overview on pre-clinical therapeutic approaches, Cardiovasc. Toxicol. 22 (2022) 292–310, https://doi.org/ 10.1007/s12012-022-09721-1.
- [4] X. Zhang, X. Li, Q. You, X. Zhang, Prodrug strategy for cancer cell-specific targeting: A recent overview, Eur. J. Med. Chem. 139 (2017) 542–563, https://doi. org/10.1016/j.ejmech.2017.08.010.
- [5] C. Souza, D.S. Pellosi, A.C. Tedesco, Prodrugs for targeted cancer therapy, Expert Rev. Anticancer Ther. 19 (2019) 483–502, https://doi.org/10.1080/ 14737140.2019.1615890.
- [6] S. Arpicco, F. Dosio, B. Stella, L. Cattel, Anticancer prodrugs: An overview of major strategies and recent developments, Curr. Top. Med. Chem. 11 (2011) 2346–2381, https://doi.org/10.2174/156802611797183221.
- [7] G. Xu, H.L. McLeod, Strategies for enzyme/prodrug cancer therapy, Clin. Cancer Res. 7 (2001) 3314–3324.
- [8] Y. Yang, H. Aloysius, D. Inoyama, Y. Chen, L. Hu, Enzyme-mediated hydrolytic activation of prodrugs, Acta Pharm. Sin. B. 1 (2011) 143–159, https://doi.org/ 10.1016/j.apsb.2011.08.001.
- [9] H.C. Hang, C. Yu, D.L. Kato, C.R. Bertozzi, A metabolic labeling approach toward proteomic analysis of mucin-type O-linked glycosylation, Proc. Natl. Acad. Sci. USA 100 (2003) 14846–14851, https://doi.org/10.1073/pnas.2335201100.
- [10] X. Xie, B. Li, J. Wang, C. Zhan, Y. Huang, F. Zeng, S. Wu, Tetrazine-mediated bioorthogonal system for prodrug activation, photothermal therapy, and optoacoustic imaging, ACS Appl. Mater. Interfaces 11 (2019) 41875–41888, https://doi.org/10.1021/acsami.9b13374.
- [11] L. Wang, P. Jing, J. Tan, C. Liao, Y. Chen, Y. Yu, S. Zhang, "One-stitch" bioorthogonal prodrug activation based on cross-linked lipoic acid nanocapsules, Biomaterials 273 (2021) 120823, https://doi.org/10.1016/j. biomaterials.2021.120823.
- [12] X. Xie, B. Li, J. Wang, C. Zhan, Y. Huang, F. Zeng, S. Wu, Bioorthogonal nanosystem for near-infrared fluorescence imaging and prodrug activation in mouse model, ACS Mater. Lett. 1 (2019) 549–557, https://doi.org/10.1021/ acsmaterialslett 9b00281
- [13] S.S. Matikonda, D.L. Orsi, V. Staudacher, I.A. Jenkins, F. Fiedler, J. Chen, A. B. Gamble, Bioorthogonal prodrug activation driven by a strain-promoted 1,3-dipolar cycloaddition, Chem. Sci. 6 (2015) 1212–1218, https://doi.org/10.1039/c4sc02574a.

- [14] B. Li, P. Liu, H. Wu, X. Xie, Z. Chen, F. Zeng, S. Wu, A bioorthogonal nanosystem for imaging and in vivo tumor inhibition, Biomaterials 138 (2017) 57–68, https:// doi.org/10.1016/j.biomaterials.2017.05.036.
- [15] R. Van Brakel, R.C.M. Vulders, R.J. Bokdam, H. Grüll, M.S. Robillard, A doxorubicin prodrug activated by the staudinger reaction, Bioconjug. Chem. 19 (2008) 714–718, https://doi.org/10.1021/bc700394s.
- [16] M.M.A. Mitry, F. Greco, H.M.I. Osborn, In vivo applications of bioorthogonal reactions: Chemistry and targeting mechanisms, Chem. - A Eur. J. 29 (2023) 1–22, https://doi.org/10.1002/chem.202203942.
- [17] A. Harduin-Lepers, V. Vallejo-Ruiz, M.A. Krzewinski-Recchi, B. Samyn-Petit, S. Julien, P. Delannoy, The human sialyltransferase family, Biochimie 83 (2001) 727–737, https://doi.org/10.1016/S0300-9084(01)01301-3.
- [18] M. Fukuda, Possible roles of tumor-associated Carbohydrate Antigens1, Cancer Res. (1996) 2237–2244.
- [19] F. Dall'Olio, M. Chiricolo, Sialyltransferases in cancer, Glycoconj. J. 18 (2001) 841–850, https://doi.org/10.1023/A:1022288022969.
- [20] D.H. Dube, C.R. Bertozzi, Glycans in cancer and inflammation Potential for therapeutics and diagnostics, Nat. Rev. Drug Discov. 4 (2005) 477–488, https://doi.org/10.1038/nrd1751.
- [21] H.Y. Yoon, M.L. Shin, M.K. Shim, S. Lee, J.H. Na, H. Koo, H. Lee, J.H. Kim, K. Y. Lee, K. Kim, I.C. Kwon, Artificial chemical reporter Targeting strategy using bioorthogonal click reaction for improving active-targeting efficiency of tumor, Mol. Pharm. 14 (2017) 1558–1570, https://doi.org/10.1021/acs.molpharmaceut.6b01083.
- [22] M.M.A. Mitry, S.Y. Boateng, F. Greco, H.M.I. Osborn, Bioorthogonal activation of prodrugs, for the potential treatment of breast cancer, using the Staudinger reaction, RSC Med. Chem. 14 (2023) 1537, https://doi.org/10.1039/d3md00137g.
- [23] R.M. Versteegen, R. Rossin, W. Ten Hoeve, H.M. Janssen, M.S. Robillard, Click to release: Instantaneous doxorubicin elimination upon tetrazine ligation, Angew. Chemie - Int. Ed. 52 (2013) 14112–14116, https://doi.org/10.1002/ anie.201305969.
- [24] L. Zuo, J. Ding, C. Li, F. Lin, P.R. Chen, P. Wang, G. Lu, J. Zhang, L.L. Huang, H. Y. Xie, Coordinating bioorthogonal reactions with two tumor-microenvironment-responsive nanovehicles for spatiotemporally controlled prodrug activation, Chem. Sci. 11 (2020) 2155–2160, https://doi.org/10.1039/c9sc05036a.
- [25] Q. Yao, F. Lin, X. Fan, Y. Wang, Y. Liu, Z. Liu, X. Jiang, P.R. Chen, Y. Gao, Synergistic enzymatic and bioorthogonal reactions for selective prodrug activation in living systems, Nat. Commun. 9 (2018) 1–35, https://doi.org/10.1038/s41467-018.07490.6
- [26] R. Rossin, R.M. Versteegen, J. Wu, A. Khasanov, H.J. Wessels, E.J. Steenbergen, W. Ten Hoeve, H.M. Janssen, A.H.A.M. Van Onzen, P.J. Hudson, M.S. Robillard, Chemically triggered drug release from an antibody-drug conjugate leads to potent antitumour activity in mice, Nat. Commun. 9 (2018) 1–11, https://doi.org/10.1038/s41467-018-03880-y.
- [27] H. Wang, R. Wang, K. Cai, H. He, Y. Liu, J. Yen, Z. Wang, M. Xu, Y. Sun, X. Zhou, Q. Yin, L. Tang, I.T. Dobrucki, L.W. Dobrucki, E.J. Chaney, S.A. Boppart, T.M. Fan, S. Lezmi, X. Chen, L. Yin, J. Cheng, Selective in vivo metabolic cell-labeling-mediated cancer targeting, Nat. Chem. Biol. 13 (2017) 415–424, https://doi.org/10.1038/nchembio.2297.
- [28] J.D. Byrne, T. Betancourt, L. Brannon-Peppas, Active targeting schemes for nanoparticle systems in cancer therapeutics, Adv. Drug Deliv. Rev. 60 (2008) 1615–1626, https://doi.org/10.1016/j.addr.2008.08.005.
- [29] C. Agatemor, M.J. Buettner, R. Ariss, K. Muthiah, C.T. Saeui, K.J. Yarema, Exploiting metabolic glycoengineering to advance healthcare, Nat. Rev. Chem. 3 (2019) 605–620, https://doi.org/10.1038/s41570-019-0126-y.
- [30] J. Chen, P. Ji, G. Gnawali, M. Chang, F. Gao, H. Xu, W. Wang, Building bioorthogonal click-release capable artificial receptors on cancer cell surface for imaging, drug targeting and delivery, Acta Pharm. Sin. B. 13 (2023) 2736–2746, https://doi.org/10.1016/j.apsb.2022.12.018.
- [31] Y.N. Malykh, R. Schauer, L. Shaw, N-Glycolylneuraminic acid in human tumours, Biochimie 83 (2001) 623–634, https://doi.org/10.1016/S0300-9084(01)01303-7.
- [32] M. Grammel, H.C. Hang, Chemical reporters for biological discovery, Nat. Chem. Biol. 10 (2014) 239, https://doi.org/10.1038/nchembio0314-239c.
- [33] D. Thomas, A.K. Rathinavel, P. Radhakrishnan, Altered glycosylation in cancer: A promising target for biomarkers and therapeutics, Biochim. Biophys. Acta - Rev. Cancer. 1875 (2021) 188464, https://doi.org/10.1016/j.bbcan.2020.188464.
- [34] R.K. Singh, S. Kumar, D.N. Prasad, T.R. Bhardwaj, Therapeutic journery of nitrogen mustard as alkylating anticancer agents: Historic to future perspectives, Eur. J. Med. Chem. 151 (2018) 401–433, https://doi.org/10.1016/j.ejmech.2018.04.001.
- [35] O. Tacar, P. Sriamornsak, C.R. Dass, Doxorubicin: An update on anticancer molecular action, toxicity and novel drug delivery systems, J. Pharm. Pharmacol. 65 (2013) 157–170, https://doi.org/10.1111/j.2042-7158.2012.01567.x.
- [36] F. Yang, S.S. Teves, C.J. Kemp, S. Henikoff, Doxorubicin, DNA torsion, and chromatin dynamics, Biochim. Biophys. Acta - Rev. Cancer. 2014 (1845) 84–89, https://doi.org/10.1016/j.bbcan.2013.12.002.
- [37] W.A. Velema, Z. Lu, Chemical RNA cross-linking: Mechanisms, computational analysis, and biological applications, JACS Au. 3 (2023) 316–332, https://doi.org/ 10.1021/jacsau.2c00625.
- [38] A. La-Venia, R. Dzijak, R. Rampmaier, M. Vrabel, An optimized protocol for the synthesis of peptides containing trans-cyclooctene and bicyclononyne dienophiles as useful multifunctional Bioorthogonal probes, Chem. - A Eur. J. 27 (2021) 13632–13641, https://doi.org/10.1002/chem.202102042.
- [39] Y. Hao, X. Fan, Y. Shi, C. Zhang, D. Sun, K. Qin, W. Qin, W. Zhou, X. Chen, Next-generation unnatural monosaccharides reveal that ESRRB O-GlcNAcylation regulates pluripotency of mouse embryonic stem cells, Nat. Commun. 10 (2019) 4065, https://doi.org/10.1038/s41467-019-11942-y.

- [40] K.G. Ozdemir, H. Yilmaz, S. Yilmaz, In vitro evaluation of cytotoxicity of soft lining materials on L929 cells by MTT assay, J. Biomed. Mater. Res. - Part B Appl. Biomater. 90 (B) (2009) 82–86, https://doi.org/10.1002/jbm.b.31256.
- [41] A.R. Aarathy, B.B. Lahiri, S.S. Pillai, J. Philip, Physicochemical properties and AC magnetic field induced heating properties of solvothermally prepared thiospinel: Fe₃S₄ (greigite) nanoparticles, Phys. Scr. 98 (2023), https://doi.org/10.1088/1402-4896/acd0e0.
- [42] X. Liu, F. Wu, K. Cai, Z. Zhao, Z. Zhang, Y. Chen, Y. Liu, J. Cheng, L. Yin, Cancer cell-Targeted cisplatin prodrug delivery: In vivo via metabolic labeling and bioorthogonal click reaction, Biomater. Sci. 9 (2021) 1301–1312, https://doi.org/ 10.1039/d0bm01709d.
- [43] J. Qiao, F. Tian, Y. Deng, Y. Shang, S. Chen, E. Chang, J. Yao, Bio-orthogonal click-targeting nanocomposites for chemo-photothermal synergistic therapy in breast cancer, Theranostics 10 (2020) 5305–5321, https://doi.org/10.7150/thno.42445.
- [44] E.M. Flefel, W.I. El-Sofany, R.A.K. Al-Harbi, M. El-Shahat, Development of a novel series of anticancer and antidiabetic: Spirothiazolidines analogs, Molecules. 24 (2019). https://doi.org/10.3390/molecules24132511.
- [45] A.H. Shamroukh, M. El-Shahat, J. Drabowicz, M.M. Ali, A.E. Rashad, H.S. Ali, Anticancer evaluation of some newly synthesized N-nicotinonitrile derivative, Eur. J. Med. Chem. 69 (2013) 521–526, https://doi.org/10.1016/j. eimech. 2013.09.005
- [46] E.M. Flefel, W.I. El-Sofany, H.M. Awad, M. El-Shahat, First synthesis for bis-spirothiazolidine derivatives as a novel heterocyclic framework and their biological activity, Mini Rev. Med. Chem. 20 (2020) 152–160.
- [47] R. Rostami, S. Mittal, P. Rostami, F. Tavassoli, B. Jabbari, Brain metastasis in breast cancer: A comprehensive literature review, J. Neurooncol. 127 (2016) 407–414, https://doi.org/10.1007/s11060-016-2075-3.
- [48] P.S. Steeg, The blood-tumour barrier in cancer biology and therapy, Nat. Rev. Clin. Oncol. 18 (2021) 696–714, https://doi.org/10.1038/s41571-021-00529-6.
- [49] Y. Wang, F. Ye, Y. Liang, Q. Yang, Breast cancer brain metastasis: Insight into molecular mechanisms and therapeutic strategies, Br. J. Cancer. 125 (2021) 1056–1067, https://doi.org/10.1038/s41416-021-01424-8.
- [50] D. Han, S. Moon, Y. Kim, H. Min, Y. Kim, Characterization of the membrane proteome and N-glycoproteome in BV-2 mouse microglia by liquid chromatography-tandem mass spectrometry, BMC Genomics 15 (2014), https:// doi.org/10.1186/1471-2164-15-95.

- [51] H. Thiesler, J. Beimdiek, H. Hildebrandt, Polysialic acid and Siglec-E orchestrate negative feedback regulation of microglia activation, Cell. Mol. Life Sci. 78 (2021) 1637–1653, https://doi.org/10.1007/s00018-020-03601-z.
- [52] M. Puigdellívol, D.H. Allendorf, G.C. Brown, Sialylation and Galectin-3 in microglia-mediated neuroinflammation and neurodegeneration, Front. Cell. Neurosci. 14 (2020) 1–11, https://doi.org/10.3389/fncel.2020.00162.
- [53] C. Lauro, C. Limatola, Metabolic reprograming of microglia in the regulation of the innate inflammatory response, Front. Immunol. 11 (2020) 1–8, https://doi.org/ 10.3389/fimmu.2020.00493.
- [54] L. Du, H. Qin, T. Ma, T. Zhang, D. Xing, In vivo imaging-guided photothermal/ photoacoustic synergistic therapy with bioorthogonal metabolic glycoengineeringactivated tumor targeting nanoparticles, ACS Nano 11 (2017) 8930–8943, https:// doi.org/10.1021/acsnano.7b03226.
- [55] M.R. Karver, R. Weissleder, S.A. Hilderbrand, Synthesis and evaluation of a series of 1,2,4,5-tetrazines for bioorthogonal conjugation, Bioconjug. Chem. 22 (2011) 2263–2270, https://doi.org/10.1021/bc200295y.
- [56] J. Šečkutė, N.K. Devaraj, Expanding room for tetrazine ligations in the in vivo chemistry toolbox, Curr. Opin. Chem. Biol. 17 (2013) 761–767, https://doi.org/ 10.1016/j.cbpa.2013.08.004.
- [57] A.C. Knall, M. Hollauf, C. Slugovc, Kinetic studies of inverse electron demand Diels-Alder reactions (iEDDA) of norbornenes and 3,6-dipyridin-2-yl-1,2,4,5-tetrazine, Tetrahedron Lett. 55 (2014) 4763–4766, https://doi.org/10.1016/j.tetlet.2014.07.002
- [58] M.F. García, X. Zhang, M. Shah, J. Newton-Northup, P. Cabral, H. Cerecetto, T. Quinn, 99mTc-bioorthogonal click chemistry reagent for in vivo pretargeted imaging, Bioorganic Med. Chem. 24 (2016) 1209–1215, https://doi.org/10.1016/ j.bmc.2016.01.046.
- [59] O. Chassany, S. Urien, P. Claudepierre, G. Bastian, J.P. Tillement, Comparative serum protein binding of anthracycline derivatives, Cancer Chemother. Pharmacol. 38 (1996) 571–573, https://doi.org/10.1007/s002800050529.
- [60] H.J. Gross, R. Brossmer, Enzymatic introduction of a fluorescent sialic acid into oligosaccharide chains of glycoproteins, Eur. J. Biochem. 177 (1988) 583–589, https://doi.org/10.1111/j.1432-1033.1988.tb14410.x.
- [61] J.E. Martin, S.W. Tanenbaum, M. Flashner, A facile procedure for the isolation of N-acetylneuramic acid from edible bird's-nest, Carbohydr. Res. 56 (1977) 423–425, https://doi.org/10.1016/s0008-6215(00)83368-6.